TALLINN UNIVERSITY OF TECHNOLOGY
SCHOOL OF ENGINEERING
Department of Materials and Environmental Technology

ELECTROSYNTHESIZED MOLECULARLY IMPRINTED POLYMER FILMS SELECTIVE TOWARDS BRAIN-DERIVED NEUROTROPHIC FACTOR

ELEKTROKEEMILISELT SÜNTEESITUD MOLEKULAARSELT JÄLJENDATUD POLÜMEERID AJU-PÄRITOLUGA NEUROTROOFSE TEGURI SELEKTIIVSEKS ÄRATUNDMISEKS

MASTER THESIS

Student: Oghenetega Allen Obewhere
Student code: 184667KAYM
Supervisor: Dr. Vitali Sõritski
Co-supervisor: Dr. Jekaterina Reut

Tallinn 2020

AUTHOR'S DECLARATION

Hereby I declare that I have written this thesis independently.
No academic degree has been applied for based on this material. All works, major viewpoints and data of the other authors used in this thesis have been referenced.

"27" May, 2020.

Author: Oghenetega Allen Obewhere
/signature /

Thesis is in accordance with the terms and requirements

"....." ..... 20….

Supervisor: Dr Vitali Sõritski
/signature/

Co-supervisor: Dr. Jekaterina Reut
/signature/

Accepted for defence

"....."..... 20… .

Chairman of theses defence commission: Prof. Marina Trapido
/name and signature/

Department of Materials and Environmental Technology

THESIS TASK

Student: Oghenetega Allen Obewhere

Study programme: KAYM09/18 Materials and Processes for Sustainable Energetics

Main speciality: Materials for Sustainable Energetics

Supervisor(s):Senior Research Scientist, Dr Vitali Sõritski (+372 6202820)

Senior Lecturer, Dr Jekaterina Reut (+372 6202820)

Thesis topic:

(in English) ELECTROSYNTHESIZED MOLECULARLY IMPRINTED POLYMER FILMS SELECTIVE TOWARDS BRAIN-DERIVED NEUROTROPHIC FACTORS

(in Estonian) ELEKTROKEEMILISELT SÜNTEESITUD MOLEKULAARSELT JÄLJENDATUD POLÜMEERID AJU-PÄRITOLUGA NEUROTROOFSE TEGURI SELEKTIIVSEKS ÄRATUNDMISEKS

Thesis main objectives:

1. Rational selection of an appropriate electropolymerizable functional monomer.
2. Optimization of electropolymerization parameters of the selected functional monomer in the presence of the target/template molecule, Brain-derived Neurotrophic Factor (BDNF) on the working electrode surface of thin film electrode (TFE).
3. Removal of BDNF from the polymer matrix using an appropriate washing out solvent and procedures to generate a BDNF-Imprinted Polymer (BDNF-MIP/TFE) on TFE;
4. Study BDNF-MIP/TFE's performance in terms of selectivity and its limit of detection (LoD) toward BDNF.

Thesis tasks and time schedule:

No	Task description	Deadline
1.	Rational selection of an appropriate electropolymerizable functional monomer.	september 2019
2.	Optimization of electropolymerization parameters of the selected functional monomer in the presence of the target/template	october 2019

	molecule, Brain-derived Neurotrophic Factor (BDNF) on the working electrode surface of thin film electrode (TFE).	
3.	Removal of BDNF from the polymer matrix using an appropriate washing out solvent and procedures to generate a BDNF-Imprinted Polymer (BDNF-MIP/TFE) on TFE.	December 2019
4	Study BDNF-MIP/TFE performance in terms of selectivity and its limit of detection (LoD) toward BDNF.	January 2020

Language: English **Deadline for submission of thesis:** "27" May, 2020

Student: Oghenetega Allen Obewhere "3" September, 2019
/signature/

Supervisor: Dr Vitali Sõritski "3" September, 2019
/signature/

Consultant: ..... ".....".....2019
/signature/

Head of study programme: Dr Sergei Bereznev ".....".....2019
/signature/

CONTENTS

PREFACE

This research and all data collected were carried out at the Laboratory of Biofunctional Materials, Department of Materials and Environmental Technology, Tallinn University of Technology. Initiation of the title was done by the author, Oghenetega Allen Obewhere with due consultation and assistance from my Supervisor, Dr. Vitali Sõritski. Data collection was also done by the author with assistance from Dr. Roman Borozniak.

I am eternally grateful to my supervisor, Dr. Vitali Sõritski for his mentorship, guidance and whose incessant patience provided me with an apt atmosphere for a successful completion of my thesis objectives. He provided insights, positively pushed me to my limits and supported me in the thesis write-up. His continuous constructive criticism proved very useful to me in academic life and laboratory work. I am also thankful to my co-supervisor, Dr. Jekaterina Reut, for her insights, strenuous efforts in reviewing, critically evaluating and unbiasedly criticizing the quality and authenticity of this work. Her feedback and reviewing allowed a successful completion of this work. My gratitude also goes to Dr. Roman Borozniak who made sure I was always active and working and was always a source of encouragement to me on the dark lonely days. I would also like to thank Dr. George Ayankojo who was always willing to lend a helping hand, proffer solutions, give directions advice and encourage me whenever I feel overwhelmed or discouraged at any point of my research work. Lastly, to my other colleagues Abdul Raziq and Chao Nguyen for making the atmosphere conducive so I could work with them.

To mitigate the increasing reports and prevalence of neurodegenerative disorders among the human population especially in the young, detection and clinical monitoring of neurotrophic factor proteins is essential. Thus, this study aims at designing an artificial (biomimetic) detection platform for the detection of brain-derived neurotrophic factor, BDNF, a neurodegenerative disorder biomarker in human serum, employing the principle of molecular imprinting.

This work was supported by the **Estonian Research Council grant (PRG307)**. Also, I cordially thank **Icosagen AS** and **Prof. M. Ustav** for providing the neurotrophic factor proteins.

Keywords: Molecularly imprinted polymers; brain-derived neurotrophic factor; neurodegenerative disorders; electrochemical sensor, master thesis.

List of abbreviations and symbols

AA	Acetic Acid
AD	Alzheimer's Disease
ADT	Autodock Tools
AE	Auxiliary Electrode
ARMET	Arginine-Rich, Mutated in Early-Stage Tumors, see MANF
ATP	4- aminothiophenol
BDNF	Brain-derived Neurotrophic Factor
CB	Competitive Binding
CDNF	Cerebral Dopamine Neurotrophic Factor
CD48	Cluster of Differentiation 48
CV	Cyclic Voltammetry
DPV	Differential Pulse Voltammetry
DTSSP	3,3'-dithiobis(sulfosuccinimidyl propionate)
EIS	Electrochemical Impedance Spectroscopy
ELISA	Enzyme-linked Immunosorbent Assay
HSA	Human Serum Albumin
LOD	Limit of detection
MANF	Mesencephalic Astrocyte-Derived Neurotrophic Factor
ME/EtOH	2-mercaptoethanol in ethanol
MI	Molecular Imprinting
MIP	Molecularly Imprinted Polymers
mPD	meta-Phenylenediamine
NF	Neurotrophic Factor
NIP	Non-imprinted Polymer
RE	Reference Electrode
PmPD	Poly(meta-Phenylenediamine)
TFE	Thin Film Electrode
WE	Working Electrode

INTRODUCTION

Over the years, the issues of dementia, depression and certain other neurological disorders (NDs) are mental health problems that are commonly encountered in neuropsychiatric practice in the elderly worldwide [1]. Although the underlying factors that contribute to the incidence and progression of these disorders might vary from oxidative stress to inflammation as well as genetic and dietary factors, the major factor is still not yet known. Nowadays, the reported cases of such NDs, particularly depression in young people is increasing and becoming prevalent at an alarming rate although under certain circumstances [2]. A group of endogenous proteins, which were first discovered in the early 1950s was seen to support the survival, growth, morphological plasticity or synthesis of proteins for differentiated functions of neurons [3]. These proteins, so-called neurotrophic factors (NFs), which includes brain-derived neurotrophic factor (BDNF), cerebral dopamine neurotrophic factor (CDNF) among others are neuroprotective in nature and their actions have been of interest and are still being studied in medical research fields. In a recent study carried out by Forlenza et al. [4], the authors showed a correlation between the presence of a decreased serum BDNF concentration and development of Alzheimer's Disease in amnestic Mild Cognitive Impaired subjects. Therefore, because there is an interrelationship between the serum concentration of these NFs particularly BDNF and the ND state of an individual, detecting their presence and measuring their concentration in serum would be significant in clinical diagnosis of the said disorder as was also reported by Balietti et al. [5].

Nowadays, a number of analytical methods for detection and quantification of NF proteins in serum, are available and include, for example, Enzyme-linked Immunosorbent Assay (ELISA), Liquid Chromatography-Mass Spectrometry, Fluorescence Spectroscopy, Size-exclusion Chromatography, and Protein Immunostaining. All of these methods, though known for their highly accurate analytical measurements, have many shortcomings including the requirement of expensive analytical grade solvents and specialized conditions for analysis, they are considered as generally too slow when rapid response is needed, and a highly experienced and skillful operator is usually needed for the equipment. Therefore, a lot of efforts are put into developing sensors capable of analyte detection with similar detection accuracy, but at the same time providing easy handling and improved stability. Sensors modified with a Molecularly Imprinted Polymer (MIP) as a synthetic recognition element can provide a valuable solution in the field.

MIPs are artificial polymeric receptors generated via Molecular Imprinting Technology, which can be defined as a process of creating specific molecular recognition sites in

polymeric matrices. MIPs are advantageous owing to the fact that they are reproducible, maintain inexpensive fabrication, and they exhibit exceptional chemical and thermal stability [6]. MIPs have been studied extensively for imprinting of proteins such as immunoglobulins [7], enzymes [8], [9], nucleic acids [10] etc.

Imprinting of a protein however, represents challenges such as preserving the protein native tertiary or quaternary state during polymer formation and reduced selectivity due to conformational flexibility [11]. Notwithstanding, a number of synthesis approaches such as epitope imprinting [12] and employing surface imprinting techniques were developed [7] to overcome these challenges.

Protein-MIPs have been successfully incorporated into sensor platforms particularly Surface Plasmon Resonance (SPR) [14], Quartz Crystal Microbalance (QCM) [13], Surface Acoustic Wave (SAW) [15] and Screen-Printed Electrodes (SPEs) [16]. Recently, Syritski`s group reported a MIP-based synthetic receptor for BDNF prepared by photopolymerization and integrated with SPE sensor for rapid Point of Care (PoC) medical diagnostic purposes [17]. However, SPEs exhibit low stability and cannot withstand rigorous cleaning procedures which make them suitable for single analysis.

Thin film electrode (TFE) on the other hand, can be a promising electrochemical sensing platform to fabricate MIP-sensor due to its stability, low cost and use of a small volume of analyte for analysis (1-5 microliters). Because its substrate is glass, it can withstand extreme treatment conditions with chemicals making it reusable after cleaning.

Electrochemical synthesis allows a simple and direct integration of a uniform polymer film with a sensor platform [18]. The electrochemical synthesis approach provides good control of the polymer thickness down to the nanometers range, the ability to carry out synthesis at room temperature, as well as the possibility to prepare MIP in a microarray format [19], [20]. Application of electropolymerization for protein imprinting have shown favorable results. Thus, Syritski`s group developed an electrochemical surface imprinting strategy using a cleavable linker for protein immobilization before electrochemical polymerization [7], [21] that was successfully applied for imprinting of CDNF [15].

In this thesis, electrochemical surface imprinting approach was adapted for the synthesis of BDNF-MIP films, which was interfaced with a TFE as a stable and low-cost electrochemical sensing platform. On the gold working surface of TFE, a thin film of Poly m-Phenylenediamine (PmPD) was electrodeposited from a monomer solution of m-Phenylenediamine (mPD). Electropolymerization parameters such as applied potential and charge density were optimized in order to generate a homogeneous surface-adhering polymer film with appropriate thickness. The electrochemically synthesized polymer on TFE was further subjected to an optimized washing out

protocol in both mercaptoethanolic and acidic solutions to remove the target molecule from its matrix giving rise to the BDNF-MIP films. Lastly, the analytical performance of the resulting BDNF-MIP/TFE was studied in terms of its sensitivity and selectivity for the target analyte, BDNF.

1. LITERATURE REVIEW

1.1 Molecular imprinting

The technology of creating artificial recognition sites in polymeric matrices which are complementary to the template in their size, shape and spatial arrangement of functional groups is known as Molecular Imprinting (MI) [6]. MI dates back to the early 1930s when a research group from Kiev, reported some unusual adsorption properties in silica particles prepared using a novel synthesis procedure [22]. Other works done by research groups such as that of Pauling and Campbell [23], Martin and Synge [24] and Morrison [25] on silica imprinting were also reported but with minor publications in the area. Nonetheless, a breakthrough in organic polymer imprinting came in the early 1970s, when Wulff and Sarhan reported on preparation of specific binding sites in vinyl polymers using covalent imprinting approach [26]. Almost a decade later, organic polymer imprinting became much more advanced when the Mosbach group presented an organic MIP using only non-covalent interactions [27]. This paved the way for the modern day molecular imprinting using a non-covalent approach. The principle of MI involves co-polymerization of cross-linking monomers and a molecular complex pre-formed between the target molecule that acts as a 'template' and functional monomers using either covalent, non-covalent or semi-covalent interactions. After template removal from the polymer matrix, specific complementary cavities (interstices) are left behind the material [28]. Fig. 1.1 is a simplified representation of the molecular imprinting principle showing monomer, template and polymer relationship.

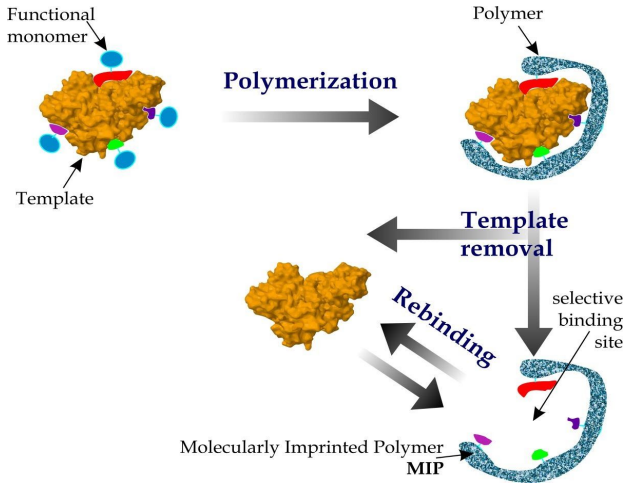

Figure 1.1 Basic principle of molecular imprinting [29]

1.1.1 Types of molecular imprinting

For the imprinting of molecules, there are different types of MI techniques that can be classified in three main categories; bulk imprinting, surface imprinting and epitope imprinting.

Bulk imprinting

In bulk imprinting a target molecule is wholly imprinted in the polymer matrix and after polymerization it is then wholly removed from the molecularly imprinted material. The main advantage of this method of imprinting is that it gives better selectivity of the polymer towards the template as the 3D shape and all functional groups of the molecule is fully imprinted. A major issue of bulk imprinting is that template molecules might be embedded too deeply in the polymer matrices and removal of the template after the polymerization process may become difficult or impossible [11]. To overcome these drawbacks, alternative imprinting techniques including surface and epitope imprinting have been developed.

Surface imprinting

In surface imprinting, the highly specific recognition sites are formed at the surface of the imprinted polymer and are more easily accessible with favorable binding kinetics [30]. This helps to address the problem of having a template molecule stuck within the rigid framework of the polymer usually encountered in bulk imprinting. In surface imprinting, less template molecules are used as compared to bulk imprinting techniques because template is only used in the surface coating step [31] which is advantageous, although this method of imprinting also has its drawback which is the possibility of lower sensitivity owing to the reduced number of imprinted sites [32]. This technique is popular and most applicable especially for imprinting of biological macromolecules and it is widely used for different types of target analytes including proteins, microbes and cells [33], [34], [35].

Epitope imprinting

The epitope approach is based on using a short peptide that represents only part of a larger peptide or protein as a template during MIP synthesis. This approach makes it possible to obtain MIPs that efficiently recognize both the template and larger peptides or proteins that possess the same C-terminal part of the structure [36].

1.2 Molecularly imprinted polymers

Molecular imprinted polymers (MIPs) - otherwise referred to as synthetic materials with specific recognition capacity for specific target molecules, have attracted much attention in the scientific world. In comparison to their biological counterparts, MIP synthetic receptors exhibit longer storage time, long-term stability in larger ranges of

pH and temperature, simplicity of use, more robust format and a relatively effortless ease of preparation [37], [38]. MIPs have been termed "plastibodies" due to their similarity to natural antibodies i.e. with respect to their ability to selectively and strongly bind a specific target molecule [39].

The potential usage of MIPs in automated detection and monitoring of a wide range of samples electrochemically, coupled with its ability to be combined with miniaturized, portable sensors, which are sensitive and selective detection platforms for analytes such as proteins, antibiotics and even cells makes MIPs quite fascinating [40]. Remarkably, the characteristics of MIPs can be modified to optimally suit a particular task and analysis medium and this also makes them very attractive candidates for performing biochemical analysis. It is therefore pertinent to carefully consider the polymer format while designing a MIP with good enough recognition for its specific template and optimal stability.

When designing a MIP for a protein target, a key parameter to consider is the noncovalent interactions between the protein and the functional monomer. These interactions are categorized into four types as is presented in Fig. 1.2: lipophilic interactions, hydrogen bonding, electrostatic interactions, and Van der waals interactions [41]. It should be noted however that imprinting of a protein molecule has its own drawbacks. One of them is the difficulty in maintaining the conformational stability of a protein molecule during the polymerization process. Moreover, the protein imprinted sites might also be attractive for smaller molecules which in turn will result in cross-reactivity and decreased selectivity of the resulting MIP.

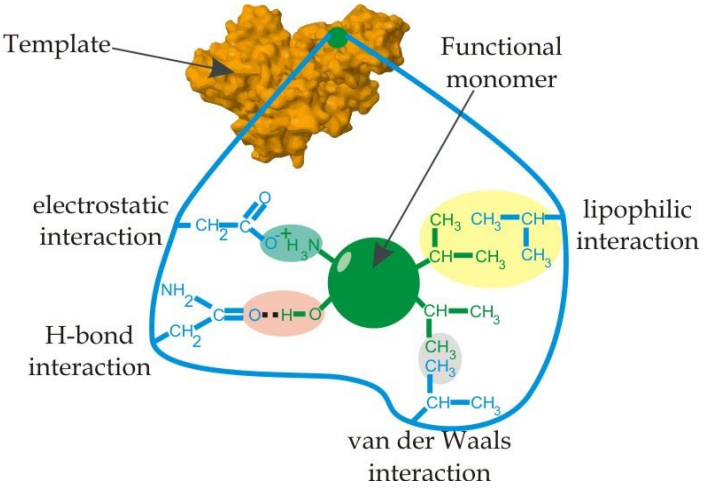

Figure 1.2 A graphical illustration of the different types of interactions in the complex between a functional monomer and a protein [42]

1.2.1 MIP formats

MIP format is a very vital aspect in MIP design and preparation and dependents on the application of the MIP. Examples of MIP formats include: monoliths, nanoparticles and thin films.

Monoliths

Monolithic MIPs are prepared by a bulk polymerization method and they are polymer blocks with template molecules enmeshed within them [43]. After preparation, the monolith polymer must further be grounded, sieved to separate particles in the range of 25-50 microns, washed thoroughly for adequate template removal and only then can it be used for experimental purposes [44]. The use of monolithic polymers is very well established especially when as columns for HPLC [45], but they have quite a number of disadvantages including: fabrication is labour-intensive and time consuming and an estimated 70% of the polymer is wasted on grinding the bulk to smaller pieces since using the monoliths just as is, is difficult [46]. Industrial scalability of monoliths is also partly not very feasible because of uneven heat distribution during post-processing of the polymer. As a result, a more thorough MIP design definitely is required to meet industrial scale.

Nanoparticles

MIP nanoparticles, with sizes ranging from 50-500 nm, possess greater surface area-to-volume ratio unlike bulk monoliths and as a result, a greater number of the selective binding sites. In addition, in the case of MIP nanoparticles the target molecules can easily access the imprinted cavities leading to the fast binding events and improving the performance in sensing and separation [47]. This format is the most suitable for surface imprinting because of the ease of accessibility to the binding sites for large molecules like proteins while the MIP surface still retains its specific recognition [39]. It's only disadvantage is that designing MIP nanoparticles can be laborious because parameters like the degree of crosslinking as well as optimum template-monomer interaction can be a limitation in the synthesis protocol [48].

Thin films

For MIP-based sensor preparation, thin polymer films are employed because they enable the production of highly uniform layers, with reproducible and easily tunable characteristics (e.g. thickness or porosity) of the resulting polymer [19]. Thin film polymers usually have thickness ranging from 0.5-30 nm and they permit rapid diffusion of ionic species in solution across the imprinted matrix which results in high and fast responses. The main advantages of this MIP format is the use of a minimal amount of protein for MIP synthesis and more easy and effective washing out procedure. One downside to this format is that thin films reduce the effective area of

the protein template available to generate interactions with functional recognition elements in the polymer when compared with bulk monolith imprints [49].

1.2.2 Electropolymerization of MIP

Electrochemical polymerization is very useful for deposition of polymer films on conducting substrate surfaces, hence permitting the possibility of integrating a uniform polymer film with a sensor platform. It is an appropriate method for MIP film synthesis because it can be carried out at room temperature and provides the possibility of a good control over the thickness of the polymer, its inner morphology and structure. The electrochemically synthesized MIPs can be applied for the preparation of MIP-based sensors [50].

1.3 Sensor platforms for MIP sensor preparation

The detection and quantification of clinically relevant molecules in patient samples during medical diagnostics or in therapeutic procedures is significant to monitor certain health conditions at an early stage. Many of traditional sensor platforms exploit the use of labelled signal detection, the examples of which include immunosensing using specific detection proteins (antibodies) with fluorescent, radio- or enzymatic labels for analyte measurement. Analysis using this platform however is time-consuming, needs specialized laboratory equipment and significant expertise to carry out, and as such currently, their application in rapid testing and point-of-care diagnosis is not very feasible [51]. Label-free methods of detection however, avoids the labelling procedure with expensive reactives, can be used to track molecular events in real time and permits more direct information to be acquired in biosensing applications [52].

MIP as a recognition element can be used in combination with a label-free sensor platform to detect the changes of response during binding on the sensor surface. Thus, MIPs were successfully integrated with various label-free sensing platforms including Surface Plasmon Resonance (SPR) [53], [54], [55], [56], Quartz Crystal Microbalance (QCM) [57], [58], [59], and SAW [60], [15], [61]. Other label-free electrochemical sensing platforms include Screen Printed Electrode (SPE) and Thin Film Electrode (TFE). Electrochemical label-free sensor platforms are advantageous in that they permit simple, rapid analytical measurements and low-cost on-field detection. They reduce the bulkiness of measurement equipment and are suitable for mass fabrication of miniaturized devices. These electrochemical sensing platforms have played a major role in the move towards simplified testing for point-of-care usage of biosensors [62]. A rather concise description of both the SPE and TFE sensor platforms are given below.

1.3.1 Screen printed electrode

Screen printed electrodes (SPEs) are sensitive, miniaturized, disposable electrodes that are produced via the screen-printed technology. Screen-printed technology consists of layer-by-layer depositions of ink upon a solid substrate, through the use of a screen or mesh. In recent years, SPEs, with low cost and ease and speed of mass production using thick film technology have been extensively employed for developing novel (electrochemical) sensing platforms and improving their performances. Increasingly, MIPs integrated with SPE sensor platforms (Fig. 1.3a) have been successfully developed for various analyte detection [17], [40], [63]. SPE usually includes a three electrode configuration (working, counter and reference electrodes) printed on either a plastic or ceramic substrate, with easily modifiable inks using inkjet printers. For SPE preparation, silver and carbon ink are commonly used pastes although other materials such as gold, platinum and silver based inks are also used. The paste material is hardened on the substrate either by firing, binding or sintering [64].

The main advantage of SPEs is the reduced sample volume required for analysis. This can be as low as a few microliters and it translates to a reduction in the overall size of the diagnostic system into which the device will be integrated. Also, SPEs are versatile because their surface can be easily modified to fit multiple purposes related to different analytes and also because they can make use of a wide range of electrochemical analysis methods for analyte detection. Lastly they can be connected to a portable instrumentation (Fig. 1.3b) which makes it possible for highly specific on-site determination of target analytes. In addition, SPEs avoid some of the common problems of classical solid electrodes, such as memory effects and tedious cleaning processes [65]. Its disadvantages however include that the sensor cannot be regenerated (single use), usually reacts destructively with thiolic solution and exhibits poor stability during electrochemical analysis.

(a) (b)

Figure 1.3 Tools for electrochemical detection on SPE sensors. (a) a SPE sensor chip, (b) a portable wireless potentiostat [66]

1.3.2 Thin-film electrode

Thin film electrode (TFE) is an electrochemical transducer prepared using thin-film technology. The technology is based on photolithography and the conducting material (mainly pure metals) is deposited (either chemical or physical vapor deposition) with a thickness of nanometers (typically 10–300 nm) [67]. The base substrate can either be glass, silicon and ceramic which gives the sensor additional mechanical stability during laboratory analyses.

TFE-based miniaturized, electrochemical sensor enables real-time detection of analytes with improved accuracy. This technology allows integration of electrochemical sensors in microfluidic devices allowing the manipulation of samples with very small volume (microliters–nanoliters range) as well as multiplexing possibility, e.g. simultaneous analysis of different analytes in a single device [68]. TFE sensors can be mass produced and a limitation of production of this sensor however is in the manufacturing process which is time-consuming with the requirement of state-of-the-art clean room facilities [69]. In this thesis MicruX™ thin film single electrode produced by MicruX Technologies (Fig. 1.4a) was used as an electrochemical transducer. This TFE is usually used together with a drop-cell connector as seen from Fig. 1.4b for easy and fast electroanalytical measurements.

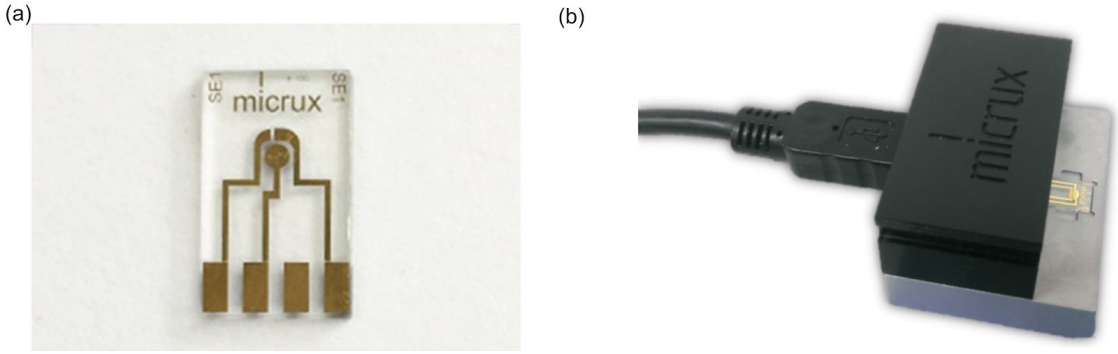

Figure 1.4 Tools for electrochemical detection on TFE (a) a micrux sensor chip, (b) micrux drop-cell connector [70]

1.4 Proteins as disease-related biomarkers

Proteins are large biomolecules, or macromolecules, consisting of one or more long chains of amino acid residues and performs a vast array of functions within organisms, including catalysing metabolic reactions, DNA replication, responding to stimuli, providing structure to cells, and organisms, and transporting molecules from one location to another. From their discovery and when they were first described in the early 19th century, their importance has been recognized by chemists including Jons Jacob Berzelius who in 1838 coined the term 'protein' from Greek proteos meaning 'holding first place'. Due to their central role in biological function, protein interactions also control the mechanisms leading to healthy and diseased states in organisms.

Diseases are often caused by mutations affecting the binding interface or leading to biochemically dysfunctional allosteric changes in proteins [71]. Therefore, protein interaction networks and their presence or absence in biofluids (such as blood serum) can elucidate the molecular basis of disease, which in turn can inform methods for prevention, diagnosis, and treatment. As a result, the concentration of the specific protein in the blood serum should be critical in the clinical diagnosis of a huge number of diseases [72].

Several serum proteins e.g human serum albumin and some members of the family of the neurotrophic factor proteins are very valuable in that apart from their basic biological functioning in the body, they can also serve as significant disease biomarkers. A description of these proteins is given in the subsequent subsections.

1.4.1 Neurotrophic factor proteins

Neurotrophic factors (NFs) are polypeptides or small proteins that support and enhance the growth, differentiation, and survival of neurons [73]. Also referred to as the nervous system growth factors (NGFs), the first protein, nerve growth factor (NGF) was discovered in the early 1950s because of its trophic effects on sensory and sympathetic neurons [74]. NFs due to their extensive influence on neurons are candidate mechanisms used for diagnosis and prognosis of neuronal and axonal disorders [75]. The correlation between different disease conditions and the concentration of neurotrophic factors (especially BDNF) in the human blood serum have been described in several literature [4], [5], [76]. Blood serum analysis which is the most widely used method for clinical diagnosis is relatively not so invasive compared with cerebrospinal fluid or brain tissue collecting but may provide significant information about the neurologic status of an individual. Of all the neurotrophins present in the healthy and diseased brain, BDNF is one of the most studied [77].

Brain-derived neurotrophic factor

Brain-derived neurotrophic factor (BDNF), discovered in 1982, is the second member of the "neurotrophin" family of neurotrophic factors. After its discovery, it was subsequently purified from a pig's brain and was shown to promote survival of a subpopulation of dorsal root ganglion neurons [78]. BDNF has a molecular weight of 14 kilodaltons (kDa) and a 3-D structure as shown in Fig. 1.5a.

In general, of all the neurotrophic factors, both BDNF and neurotrophin-4 (NT-4) have more than 50% amino acid homology. They preferentially bind tyrosine kinase receptor B (trkB) neurotrophin receptor and they are expressed extensively in the adult and aged brain [79].

The concentration of BDNF in normal human serum ranges between 8 to 40 ng/mL [80]. Regarding the level of expression of BDNF in the brain, there have been

detection of high levels of this protein in the hippocampus, amygdala, cerebellum and cerebral cortex in both rodents and humans with the highest levels found in the hippocampal neurons, while low levels have also been detected in organs such as heart, liver, lung among others [81]. It was reported that serum concentrations of BDNF varied either due to the presence of some certain neurologic disorders (NDs) such as Alzheimer's, Parkinson's disease, depression or dementia and also in patients under certain medications, most especially antidepressants. According to Forlenza et al., in people that progressed from Mild Cognitive Impairment to Alzheimer's disease, their serum level of BDNF was observed to be approximately 10 times lower than normal serum level [4]. While Toyooka et al. [82] reported serum BDNF levels in schizophrenic patients to be approximately 4 times lower than that of healthy patients. Furthermore, Lang et al. [83] showed a negative correlation of BDNF serum concentrations and neuroticism in healthy volunteers. They suggested that low BDNF levels in healthy humans with depressive personality traits might be reflective of a genetic profile, which is linked to depression and as such BDNF serum concentrations serve as a risk marker.

Mesencephalic astrocyte-derived neurotrophic factor

Mesencephalic astrocyte-derived neurotrophic factor (MANF) is an 18 kDa molecular weight protein, also known as ARMET (arginine-rich, mutated in early stage tumors) [84], and a 3-D structure as shown in Fig. 1.5b. It enhances the survival of embryonic midbrain dopaminergic neurons in vitro [85]. It also protects neurons against cerebral ischemia in vivo, possibly by inhibiting cell necrosis/apoptosis in the cerebral cortex [86]. MANF has no sequence homology to BDNF and its expression is widespread in the nervous system and non-neuronal tissues [85]. It is localized mainly to the lumen of endoplasmic reticulum (ER) and their primary function appears to be modulation of the unfolded protein response (UPR) pathway. In the brain, relatively high MANF levels have been detected in the cerebral cortex, hippocampus and cerebellar Purkinje cells [87], [88].

Cerebral dopamine neurotrophic factor

Cerebral dopamine neurotrophic factor (CDNF) also known as 'ARMET-like protein 1' is a protein with 8 conserved cysteine residues that in humans is encoded by the CDNF gene and expressed in several tissues of mouse and human, including the mouse embryonic and postnatal brain [89].

Having also a molecular weight of 18 kDa, it is a homolog to MANF, and it is structurally and functionally different from other NF proteins known to man [90], [91]. The 3-D structure of CDNF is shown below in Fig. 1.5c. In various animal models of Parkinson's disease (PD), CDNF is efficient in protecting and repairing dopaminergic neurons, and it inhibits ER stress, neuroinflammation, and apoptosis [92]. Just like

MANF, CDNF is also localized to the lumen of ER and it also functions primarily in the modulation of the UPR pathway [88].

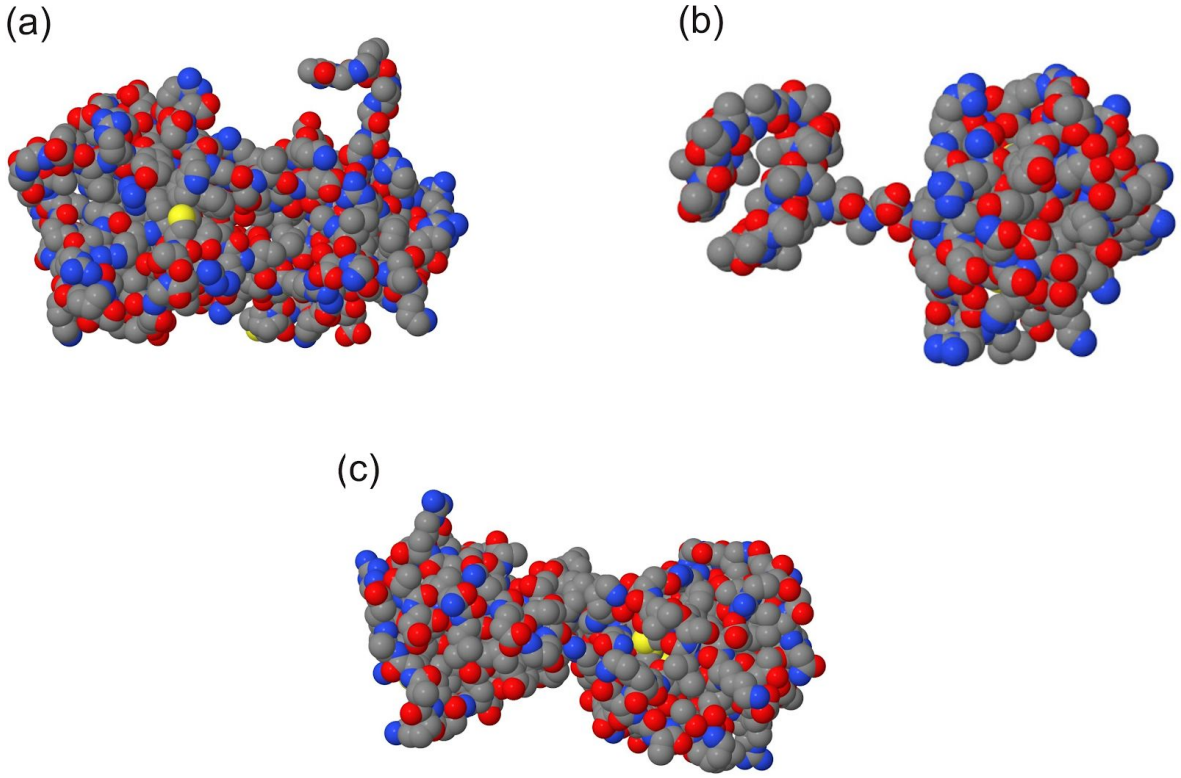

Figure 1.5 3D structure of (a) BDNF(1B8M.pdb) (b) MANF(2W51.pdb) (c) CDNF(4BIT.pdb) proteins

1.4.2 Serum proteins

Serum proteins are proteins present in blood that serve many different functions, including transport of lipids, hormones, vitamins, and minerals in the circulatory system and the regulation of acellular activity and functioning of the immune system. Other blood proteins act as enzymes, complement components, protease inhibitors, or kinin precursors. Although serum proteins have very high concentrations, they exhibit an uneven distribution in terms of composition. That is, only about 22 proteins account for 99% of all the serum proteins and these include serum albumin, globulins, and fibrinogen [93], [94]. The normal serum protein level is 6 to 8 g/dl. Albumin makes up 3.5 to 5.0 g/dl, and the remainder is the total globulins [72].

Human serum albumin

Human serum albumin (HSA), also simply referred to as albumin, is the monomeric serum albumin found in human blood (Fig. 1.6a). Albumin is the most abundant protein found in human blood plasma and it makes up more than half of the total protein present in serum. Its molecular mass is 66.5 kDa.

In serum, the reference range for albumin concentrations is approximately 35–50 mg/mL (i.e. 3.5–5.0 g/dL) [95] and it has a serum half-life of approximately 21 days [96].

Cluster of differentiation 48

Cluster of differentiation 48 (CD48) antigen also known as B-lymphocyte activation marker (BLAST-1) or signaling lymphocytic activation molecule 2 (SLAMF2) is a protein with molecular weight of about 45 kDa and a 3-D structure is shown in Fig. 1.6b. CD48 is a member of the immunoglobulin superfamily (IgSF) and it is found on the surface of lymphocytes and other immune cells, dendritic cells and endothelial cells, and it participates in the activation and differentiation pathways in these cells [97], [98].

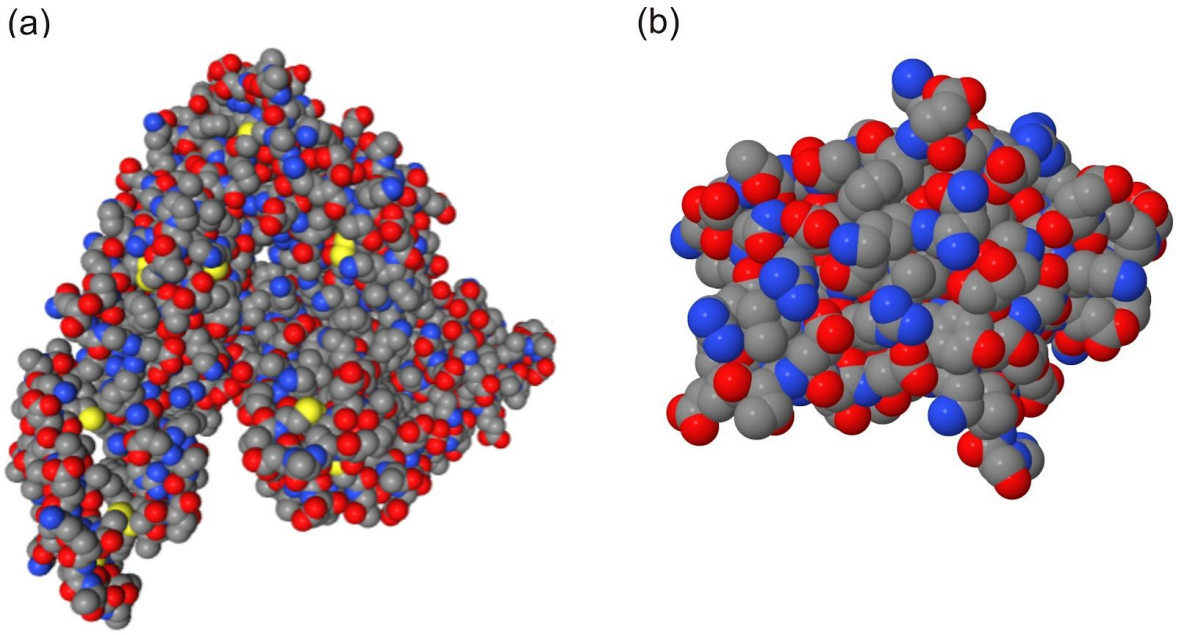

Figure 1.6 3-D structure of (a) HSA (monomeric form, 1E78.pdb) (b) CD48 (2PTV.pdb) proteins

1.5 Electrochemical methods of analysis

Different qualitative and quantitative analytical methods are available and being applied in MIP characterization. These methods namely chromatography, mass spectrophotometry, amongst others have been well established and widely used. Along with these techniques, electrochemical methods of analysis such as cyclic voltammetry, differential pulse voltammetry, electrochemical impedance spectroscopy have been shown promising and useful for MIP study [99]. The above mentioned electroanalytical methods will be discussed further below.

1.5.1 Cyclic voltammetry

Cyclic voltammetry (CV) is a versatile electroanalytical technique for the study of electroactive species and it is a very effective technique because of its capability to

rapidly observe oxidation-reduction (redox) behavior of an electrode surface, compound or biological material over a wide potential range [100]. Information about the redox potential and the electrochemical reaction rates are obtained by sweeping the voltage between two values at a fixed scan rate (Fig. 1.7 A-D) i.e. once the higher voltage limit (D) is achieved, the scan is reversed, and the voltage is swept back to its lower limit (Fig. 1.7 D-G) [101], [102].

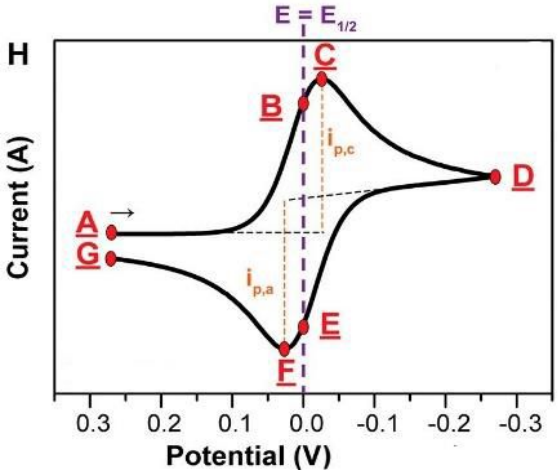

Figure 1.7 Cyclic voltammogram [103] (A G): Initial potential applied (A), Oxidation peak (C), Higher potential limit (D), Reduction peak (F) and points (B and E) corresponds to the halfway potential between the two observed peaks (C and F)

This voltage sweep produces voltammograms or cyclic voltammograms with peaks which correspond to oxidation and reduction of the analysed species respectively. Due to the inaccurate measurement of the peak currents, CV is not suited for quantitative determinations, but rather for qualitative ones, specifically the characterization of the imprinted surface [104]. The equilibrium established between the oxidized (Ox) and reduced (Red) species is described by the Nernst equation (Eq. 1.1). This equation relates the potential of an electrochemical cell (E) to the standard potential of a species (E^0) and the relative activities of the oxidized [Ox] and reduced [Red] analyte in the system at equilibrium:

$$E = E^0 + \{(RT/nF)\cdot ln([Ox]/[Red])\} \quad (1.1)$$

where F is Faraday's constant, R is the universal gas constant, n is the number of electrons, and T is the temperature.

1.5.2 Differential pulse voltammetry

Differential pulse voltammetry (DPV) is voltammetric technique, which exploits pulses of fixed amplitude superimposed on a slope of increasing potential that are applied at

constant interval to the working electrode (WE) of an electrochemical sensor [105], [106]. Current is measured before the application of the pulse and after the second pulse. By sampling the current at the end of the successive potential pulses and plotting the current difference versus the potential, a peak-shaped response-a Gaussian graph is obtained (Fig. 1.8). The area of this peak is directly proportional to the analyte concentration. DPV is a widely used technique for quantitative measurements in electrochemical analysis due to its high sensitivity and accuracy, great peak resolution, fast measurement time and quenching of background effects [104], [107].

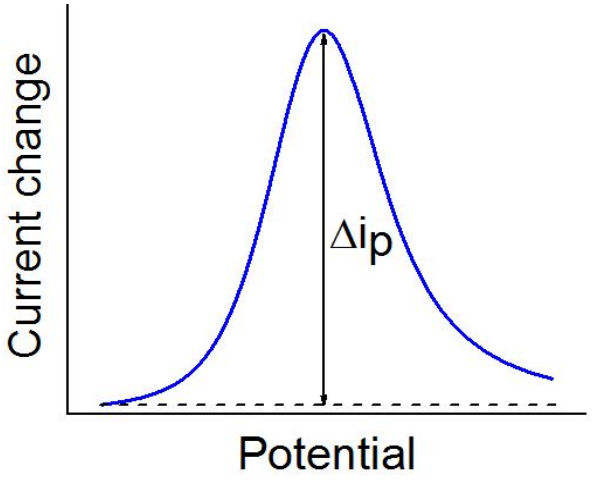

Figure 1.8 A typical DPV curve showing the change in current vs potential. Δi_p represents the change in current peak

1.5.3 Electrochemical impedance spectroscopy

For studying the impediment towards electron transfer reactions of surface-modified electrodes, electrochemical impedance spectroscopy (EIS) is a very useful tool [108]. EIS is widely used in the study of anticorrosion coatings, sensors, semiconductors, electro-organic synthesis, etc. It gives insight into the insulating properties of surface assembled monolayers (SAMs) [109]. For a well ordered SAM on an electrode, the impedance can be interpreted by an equivalent circuit of double layer capacitance in series with solution resistance. Ideally this double layer capacitance (C_{dl}) behaves like constant phase element (CPE) having the impedance (Z):

$$Z_{CPE}(\omega) = C^{-1}(\omega)^{-\alpha} \qquad (1.2)$$

where C is capacitance (measured in Farads, F), ω is angular frequency (measured in rad/s, ω=2□f where f is the frequency, Hz) and α equal to 1 (for an ideal capacitor). Usually, real systems do not necessarily behave ideally with processes that occur distributed in time and space, as a result, specialized circuit elements are often used.

These include the generalized constant phase element (CPE) and Warburg element (Z_W). The Warburg impedance is an element corresponding to the semi-infinite linear diffusion or mass transport impedances in an electrochemical system [110]. Simple equivalent electrical circuits models are used to elucidate the properties of the materials that are being studied (Fig. 1.9a).

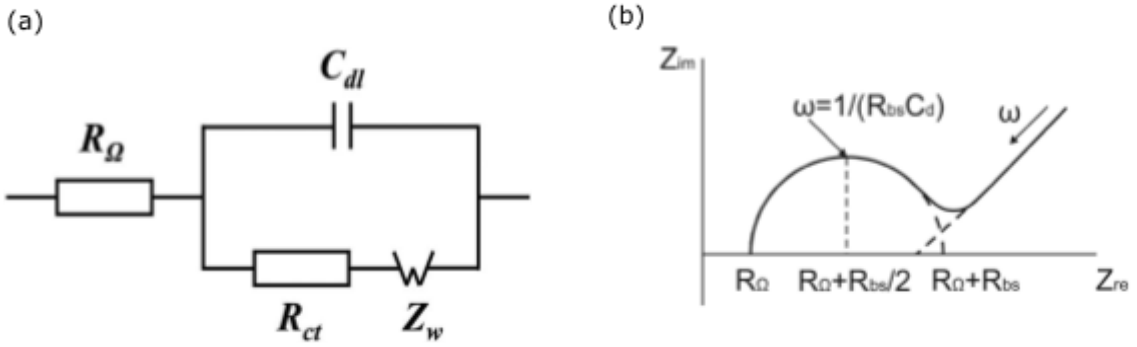

Figure 1.9 (a) Equivalent circuit model showing the Warburg impedance (Z_W), double layer capacitance (C_{dl}), ohmic resistance (R_Ω) and charge transport resistance (R_{ct}) for EIS analysis [111] (b) Nyquist plot between imaginary and real part of impedance

The complex response of the system is usually displayed as a "Nyquist plot" where the imaginary part of impedance (Z_{im}) is plotted vs. real part of the impedance (Z_{re}) as given above in (Fig. 1.9b). In this case, the semicircle has a center $Z' = R_\Omega + R_{bs}/2$ with radius R_{bs} /2.

The whole diagram demonstrates the presence of kinetic control (semicircle), and the diffusion controlled region (straight line). R_{bs} is large if the system is kinetically slow, and then there is only a limited region where mass transfer is significant. If R_{bs} is small however, then the system is kinetically facile. The charge transport resistance (R_{ct}) value represented by the diameter of the semicircle on the Nyquist plot specifies the extent of blocking of the electron transfer between the electroactive species in solution and electrode surface.

1.6 Summary of the literature review and study objectives

Since their discovery, proteins have been shown to be biologically relevant macromolecules and their presence in serum could be an important biomarker for the disease state of an organism. Since the serum concentration of a NF protein, BDNF, has been shown to have a correlation with certain neurodegenerative disorders that affect the olderly and in recent times younger people, then its detection is of particular interest in biomedical and clinical diagnostics. Present detection methods for fast analyte recognition and further quantification of the compound in a sample or mixture

today are very costly, requires the use of specialized and high grade analytical grade solvents and these systems are somewhat difficult to maintain. Therefore, biotechnological engineers are continuously investigating new methods for a cheaper, faster, and more reliable method of protein detection in biological samples.

Sensors with synthetic receptors as recognition elements, which are cheap, easy to prepare and stable, as compared to the biological receptors may be a suitable analytical tool for protein detection. Molecular imprinting is widely recognized as a prospective method to prepare these tailor-made recognition elements, so called molecularly imprinted polymers (MIPs). Today, MIPs are being studied worldwide by many research groups for their applications including solid phase extraction, catalysis, remote pollutant detection, as well as analyte-specific recognition layers in biosensors among others. The MIP can be electrochemically synthesized as a thin film directly on the conducting surface of a sensor transducer using a surface imprinting approach. This approach leads to the formation of a polymer with imprinted cavities located at or close to the surface of MIPs, enabling easy access of the target protein, and it is a promising way to overcome some of the difficulties associated with protein imprinting. Furthermore, the use of electropolymerization for polymer matrix formation is an especially attractive method for MIP film synthesis directly on a sensor transducer surface because it is a rapid process and gives a film of controlled thickness.This electrochemical sensor platform allows for analytical studies and selective characterization of the MIP films.

Recently, Syritski's group reported a BDNF-MIP prepared via photopolymerization on SPE. This BDNF-MIP/SPE, though portable, inexpensive, easy to use and permitting fast and accurate measurements still requires better stability, sensitivity and reusability. Therefore, this thesis work is purposed to be an improvement of the stability, measurement accuracy and ultimately the reusability of BDNF-MIP sensor using a different sensor platform such as thin film electrode (TFE).

The aim of the thesis is to prepare a BDNF-MIP film in TFE for the electrochemical detection of BDNF and to study the resulting BDNF-MIP electrochemical sensor in terms of its sensitivity to and selectivity for the target. The specific aims are listed below:

1. To adapt the electrochemical surface imprinting approach for preparation of BDNF-MIP films taking into account polymerization parameters such as charge density and applied potential.
2. To use thin-film gold electrodes (TFE) as a stable and low-cost electrochemical sensing platform.
3. To apply DPV technique to study the resulting BDNF-MIP/TFE electrochemical sensor in terms of its sensitivity to and selectivity for the target.

2. EXPERIMENTAL

2.1 Materials and chemicals

4-aminothiophenol 97% (ATP), 2-mercaptoethanol 99%, meta-phenylenediamine (mPD), Acetic acid 99.8% and human serum albumin (HSA, 66.5 kDa) were obtained from Sigma-Aldrich. 3,3'-dithiobis(sulfosuccinimidyl propionate) (DTSSP) was obtained from Pierce Biotechnology, ThermoFisher Scientific Inc. Ethanol 96% was obtained from Estonian Spirit OÜ (Estonia). Human recombinant BDNF (13.5 kDa, pI 9.43), CDNF (18.5 kDa, pI 7.68), MANF (18.1 kDa, pI 8.55), and CD48 antigen (cluster of differentiation 48, 22.2 kDa, pI 9.36) were supplied by Icosagen AS (Tartu, Estonia). Ultrapure water (with resistivity of 18.2 MΩ·cm, Millipore, USA) was used in the preparation of all aqueous solutions. Phosphate Buffered Saline (PBS) solution with molar concentration 0.01 M and pH value 7.4 was used to prepare analyte solutions. MicruX™ thin film electrodes (TFE) were obtained from Micrux Technologies [Gijón (Asturias), Spain]. TFE consists of a working electrode (WE) (1 mm diameter), a reference electrode (RE), and an auxiliary electrode (AE) all made of gold.

2.2 Functional monomer selection

Functional monomer for the preparation of BDNF-MIP film with optimal performance was selected based on the prediction of binding energy potential between the monomer and BDNF using computational modelling. Several electropolymerizable monomers containing complementary functional groups were randomly selected as candidate monomers. These include dopamine (DA), 3,4-ethylenedioxythiophene (EDOT), 2-aminopyridine (2AP), scopoletin and m-Phenylenediamine (mPD).

2.2.1 Molecular docking

Molecular docking procedures with Autodock 4.2.6 (from the Scripps Research Institute) were applied to selected center atoms and whole protein (receptor) rigid grid boxes. All of the analysed proteins have three dimensional (3-D) ligand-bound X-ray crystal structures available in the Protein Data Bank (PDB) and as such, BDNF, HSA, and CD48 3D structures were adopted from the PDB. The candidate monomers were scored into the protein as flexible-ligands. The monomers and the proteins were first converted to autodock tools format (into .pdbqt files) and the initial files for grid-box (.gpf) along with the docking procedure (.dpf) were prepared with autodock tools and processed with Autodock 4.2.6 software.

2.3 BDNF-MIP film preparation

BDNF-MIP film synthesis on the surface of the WE of TFE includes the following stages (Fig. 2.1): (a) functionalization of the sensor surface with 4-ATP, then DTSSP crosslinker and finally immobilization of the BDNF protein via the crosslinker; (b) electropolymerization of mPD to form a thin layer PmPD film around BDNF molecule (PmPD-BDNF); (c) removal of BDNF from the polymer matrix to form BDNF-MIP film on the sensor surface.

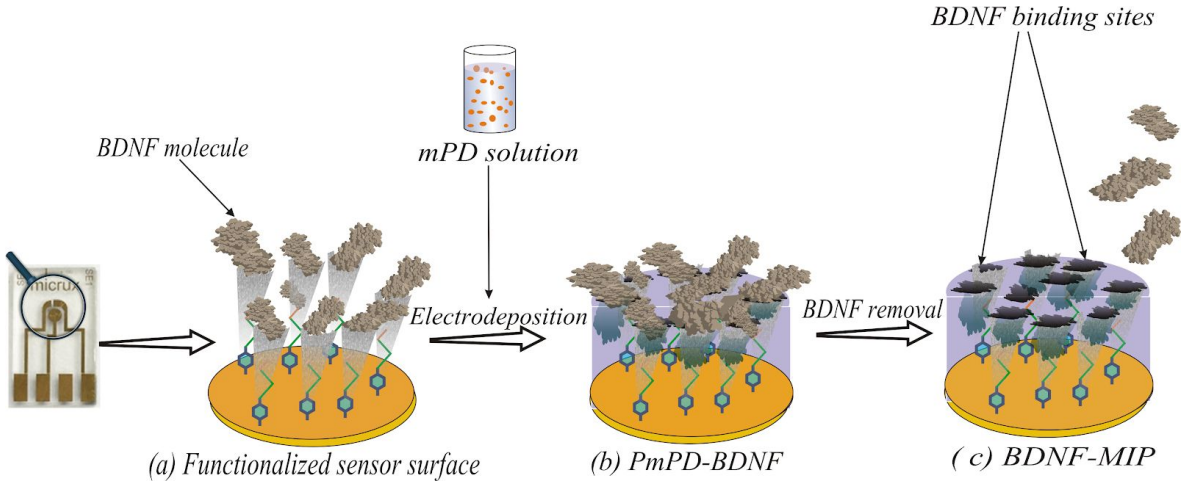

Figure 2.1 Schematic representation for BDNF-MIP film formation techniques on the Au WE of TFE. (a) Functionalization of the gold (Au) sensor surface with BDNF via DTSSP linker; (b) mPD electrodeposition; (c) removal of (washing out) BDNF from the polymer matrix to form BDNF-MIP

2.3.1 Functionalization of the sensor surface and BDNF immobilization

Prior to film electrodeposition, the working electrode (WE) of TFE was cleaned electrochemically in 0.1 M H_2SO_4 solution, cycling the potential from 0.1 to 1.15 V at a scan rate of 100 mV/s for 15 cycles. Next was WE surface modification with 4-ATP, carried out by immersing the cleaned electrode in an ethanolic solution of 0.1 M 4-ATP for a duration of 1 hour to form the self-assembled monolayer, at which point ethanol was used to assiduously rinse the electrode so as to remove the unreacted thiols at the electrode surface and then the electrode was dried under a nitrogen flow. Afterwards, the 4-ATP monolayer was further functionalized by reacting the surface with a 10 mM solution of DTSSP in PBS for approximately 30 minutes. Lastly, a 0.025 M solution of BDNF in PBS was applied to the surface for approximately 30 minutes to immobilize BDNF on the ATP-DTSSP-modified TFE [7].

2.3.2 PmPD electrodeposition

Following the BDNF immobilization on the WE of TFE the electropolymerization of mPD was done by applying a constant potential (0.6 V vs Ag/AgCl/KCl_{sat}) to the electrode immersed in PBS solution containing 10mM of mPD. The PmPD electrodeposition was carried out in an electrochemical cell connected to the Gamry workstation (Reference 600, Gamry Instruments, USA) through a connector purchased from Micrux Technologies [Gijón (Asturias), Spain]. A three-electrode external system was used, with the gold electrode of TFE as WE, a platinum wire as auxiliary electrode, and Ag/AgCl/KCl as a reference electrode.

The thickness of the electrodeposited PmPD film containing BDNF (PmPD-BDNF) was controlled by the amount of the electrical charge passed through the WE.

2.3.3 Removal of target

The target protein, BDNF, embedded within the polymer matrix of PmPD-BDNF was removed from the polymer in order to create a BDNF-MIP. To do this, the PmPD-BDNFmodified electrode was dipped in a 0.1 M solution of 2-mercaptoethanol in ethanol (ME/EtOH), and agitated using vortex at 600 rpm overnight (ca 16 hours). After rinsing with ethanol and Millipore water, the electrode was then immersed into a 3 M acetic acid (AA) solution and the same parameters of agitation were applied but for 30 minutes. Lastly, the electrode was then immersed in PBS solution for another 30 minutes without agitation. Thereafter, the resulting BDNF-MIP sensor was cleaned thoroughly with Millipore water before protein rebinding studies. To study and quantify the affinity of BDNF-MIP towards BDNF molecules, we also prepared a non-imprinted polymer (NIP) structure. Formation of BDNF-NIP was based on the very same protocol and conditions as the BDNF-MIP, excluding protein subsequent removal after polymerization. In this case there were no molecular cavities on the NIP film surface because the target protein was still very much contained in it.

2.4 Characterization of MIP preparation steps

Electrochemical measurements (CV, DPV and EIS) were used to characterize the BDNF-MIP preparation steps. The measurements were made in an electrochemical cell connected to the Gamry workstation (Reference 600, Gamry Instruments, USA) through a connector purchased from Micrux Technologies [Gijón (Asturias), Spain]. A three-electrode external system was used, with the gold electrode of TFE as WE, a platinum wire as an auxiliary electrode, and Ag/AgCl/KCl as a reference electrode during the synthesis step of the MIP preparation. All potentials in the text are referred to Ag/AgCl/KCl electrodes.

2.4.1 Cyclic voltammetry

CV measurements were carried out in a 1M KCl solution containing 4mM redox probe - $K_3[Fe(CN)_6]/K_4[Fe(CN)_6]$. The potentials were varied between -0.1 and 0.5 V at a scan rate of 50 mV/s. Three potential scan cycles were applied for each electrode.

2.4.2. Differential pulse voltammetry

The DPV measurements were conducted in 1M KCl solution containing 4mM redox probe $K_3[Fe(CN)_6]/K_4[Fe(CN)_6]$. The potentials were varied in the range of -0.2 to 0.05 V and pulse size of 0.25 mV. The pulse amplitude was 0.025 V, pulse time 0.05 s, and step potential of 0.005 V.

2.4.3 Electrochemical impedance spectroscopy

EIS measurements were performed in a 1 M KCl solution containing 4 mM redox probe $K_3[Fe(CN)_6]/K_4[Fe(CN)_6]$ solution. The frequency range was between 100 kHz and 0.1 Hz and an amplitude 10 mV was applied. The experiments were repeated for at least three times and the impedance spectra were fitted to an equivalent electrical circuit by using the equivalent circuit program provided by Gamry Echem Analyst software.

2.5 Rebinding study

The capacity of the synthesized BDNF-MIP film to specifically adsorb BDNF was analysed using DPV technique in 1 M KCl solution containing 4 mM of the redox probe $K_3[Fe(CN)_6]/K_4[Fe(CN)_6]$. After preparation the BDNF-MIP/TFE was incubated in a PBS buffer solution of pH 7.4 for 30 minutes. Thereafter, a series of DPV measurements were carried out in redox probe solution to obtain a stable baseline response, i.e. DPV response after incubation in blank PBS solution. Then, the sensor was subsequently incubated in the analyte solution of varying concentrations of BDNF from 1 to 100 ng/ml in PBS. Each analyte incubation was done for a duration of approximately 30 minutes followed by subsequent incubation in PBS for yet another 30 minutes to wash off loosely bound non-specific target analytes before the DPV measurements. The recorded DPV current peaks were normalized to obtain the normalized response signals (I) of the BDNF-MIP/TFE sensor. Eq. 2.1 below, shows the relationship between the normalized response signals (I), the initial current response after incubation in blank PBS solution (I_{PBS}) and the current response after incubation in PBS containing a particular concentration of analyte (I_{Conc}).

$$I = (I_{PBS}-I_{Conc})/I_{PBS} \quad (2.1)$$

On BDNF-NIP films as well, similar rebinding measurements were carried out with the NIP films acting as reference against MIP.

Furthermore, equilibrium adsorption isotherms were generated to determine the adsorption capacity of BDNF-MIP and -NIP against BDNF. Langmuir adsorption model as depicted in Eq. 2.2 was adopted to fit the binding isotherm and from that, both the dissociation constant (K_D) and maximum binding response at saturation (A_{sat}) values were obtained.

$$A = (A_{sat}C)/(K_D+C) \tag{2.2}$$

From the maximum binding response at saturation (A_{sat}) on BDNF-MIP and -NIP estimated, The imprinting factor for BDNF (IF_{bdnf}) can be calculated from the equation 2.3 below:

$$IF_{bdnf} = A_{sat}MIP_{target}/A_{sat}NIP_{target} \tag{2.3}$$

where $A_{sat}MIP_{target}$ and $A_{sat}NIP_{target}$ are normalized saturated response signals after BDNF (target) adsorption on BDNF-MIP and NIP films, respectively

2.6 Selectivity study

BDNF-MIP's ability to selectively recognize BDNF in buffer solutions was examined. This was done by comparing BDNF-MIP responses towards BDNF and other different proteins at concentrations from 1 - 50 ng/mL. Proteins used in the selectivity experiments include CDNF, MANF and CD48 (Fig. 1.5 and 1.6). Their selection was based on both close and slightly different similarities with the target; and also the possibility of being located in human serum same as BDNF. On BDNF-MIP and NIP, the adsorption experiments with the non-target proteins provided their A_{sat} values which were obtained by fitting the isotherm to the Langmuir model in eq. 2.2 and from that the IF' of the other proteins were calculated. Specifically, a selectivity parameter, alpha (α), which is the 'selectivity factor' given by the equation below (Eq. 2.4) was then determined.

$$\alpha = IF_{bdnf} / IF'_{non\text{-}target} \tag{2.4}$$

where IF_{bdnf} is BDNF's imprinting factor (from eqn. 2.3) and $IF'_{non\text{-}target}$ is the non-target proteins imprinting factor obtained via adsorption experiments on BDNF-MIP and NIP films, respectively.

It should be noted that for BDNF (being the target protein for BDNF-MIP in this study), its α value is approximately 1.00. Since an inverse relationship exists between the $IF'_{non\text{-}target}$ and α, it translates that a higher α value means lower polymer selectivity (or molecular recognition ability of the BDNF-MIP film) towards the individual particular non-target protein molecule and vice versa.

3. RESULTS AND DISCUSSION

3.1 Selection of functional monomer

Prior to BDNF-MIP synthesis, rational selection of the monomer was done on the basis of molecular docking [112] to determine both the energetically favorable binding positions and also the strength of the non-covalent interactions between the target molecule and a functional monomer. Molecular docking is a key tool in drug design and structural molecular biology. Its goal is to predict the predominant binding mode(s) of a ligand (a protein or any other molecule) with another protein of known three-dimensional structure [113] and it has been extensively applied for the rational selection of monomers for protein-MIPs [42], [114]. Ligand—protein docking is being explored because it can be used to perform virtual screening on large libraries of compounds, rank the results, and propose structural hypotheses of how the ligands interact with the protein.

GScore is an empirical scoring function (Eq. 3.1) which scores the energy-minimized poses of these monomers and approximates the monomer binding free energy, bearing in mind parameters such as van der Waals (vdW) interaction, electrostatic (Coul) attractions, H-bonds, solvatation effect (Desolv) and rotatable bonds energy (Tors) [42].

$$\Delta GScore = vdW + Coul + H\text{-}bond + Desolv + Tors \tag{3.1}$$

where vdW - van der Waals, Coul - electrostatic , H-bond - hydrogen bonds, Desolv - solvation effects, Tors - rotatable bonds energy respectively. It is important to note that the specific term that accounts for the solvation effect is already included in GScore [112]. For BDNF-MIP formation, the particular monomer that produced the lowest-energy (GScore) docked complex with BDNF was considered as the most suitable. According to the results obtained, mPD was seen to be the monomer with the lowest GScore value (Table 3.1) when compared with other monomers; EDOT, 2AP, scopoletin and DA (Fig. 3.1).

In addition to the computational modelling, the physical properties of a monomer such as solubility and electrooxidation potential should be considered as well in order to select the appropriate monomer for a target protein. Thus, mPD exhibits outstanding solubility in PBS meanwhile EDOT and scopoletin are less soluble in aqueous ionic solution. In comparison with DA, mPD has a faster electropolymerization rate [21] which is very valuable because in this case the immobilized protein is less prone to the synthesis solution as well as to the applied potential and so reduces the likelihood of

the protein molecule undergoing changes in its conformation in solution. For this purpose, mPD was rationally selected for BDNF-MIP synthesis.

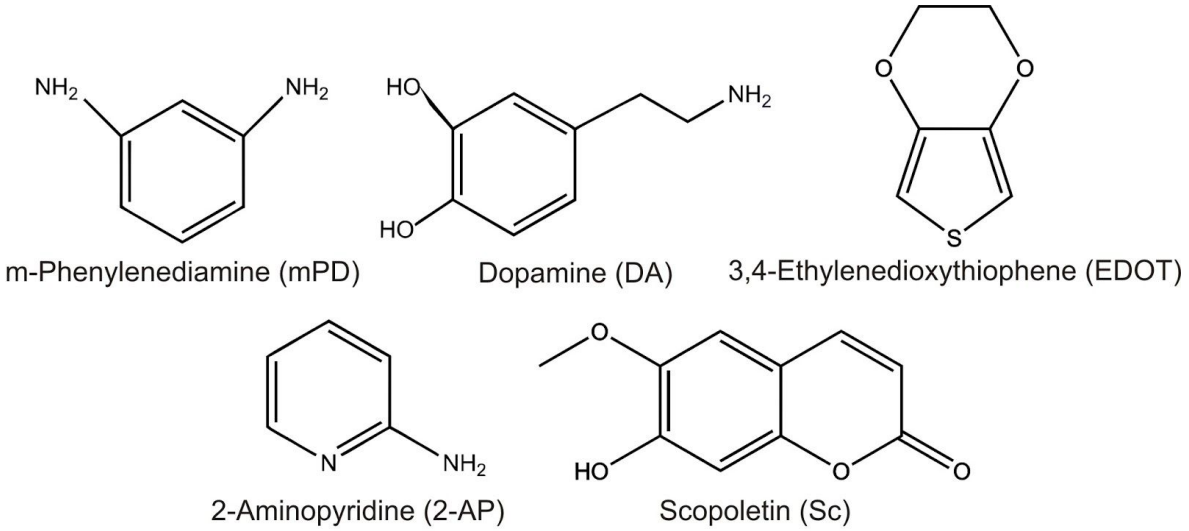

Figure 3.1 The chemical structures of the candidate monomers.

Table 3.1 shows the different selected monomers and their individual binding energy values with BDNF in decreasing order from right to left.

	GScore (kJ/mol)				
Monomers	mPD	EDOT	Scopoletin	2AP	DA
Binding energies	-22.6	-21.5	-21.46	-21.26	-19.7

3.2 BDNF-MIP preparation

The BDNF-MIP film synthesis was done electrochemically on the WE of TFE. First, the gold WE surface was modified with amino groups of 4-ATP forming a self-assembled monolayer, followed by attachment of a homobifunctional crosslinker with a cleavable disulfide bond (-S-S-), DTSSP, and lastly the immobilization of BDNF by the formation of covalent amide bond between the succinimide group of DTSSP and amino group of lysine residues of BDNF [7].

CV, DPV and EIS measurements were carried out to characterize the stages of electrode modification in the course of BDNF immobilization on the WE of the TFE. In Fig. 3.2a, the redox peak current decreases significantly after BDNF immobilization as compared to the Au surface because as a consequence of the immobilized structure (ATP-DTSSP-BDNF) on the Au surface, a dense insulating layer is created which greatly inhibits the faradaic process on the electrode surface.

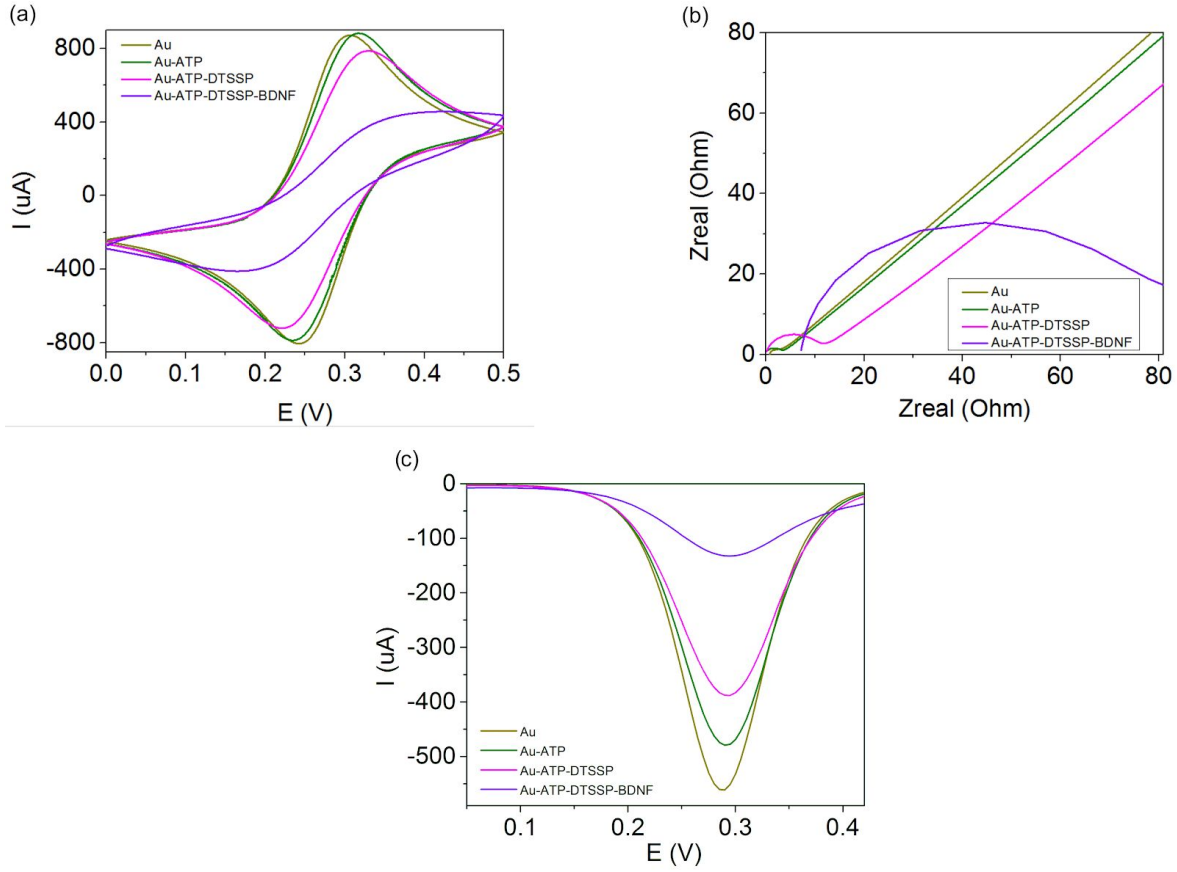

Figure 3.2 BDNF immobilization on the gold slide electrode as WE (Ag/AgCl/KCl as RE, and spiral shaped Pt as AE). Each step was characterized by (a) CV (b) EIS and (c) DPV in 1 M KCl solution containing 4 mM of the redox probe $K_3[Fe(CN)_6]/K_4[Fe(CN)_6]$

A similar result was also observed by DPV with the peak value dropping towards the baseline (point zero), after PmPD-BDNF film formation (Fig. 3.2c). For EIS, we estimate the charge transfer resistance from the width of the Nyguist plot (Fig. 3.2b). As can be seen, the width of the semicircle increased from 0.356 Ω/cm^2 (the bare Au electrode) to 0.938 Ω/cm^2 (Au-ATP), then 10.076 Ω/cm^2 (Au-ATP-DTSSP) and lastly 65.56 Ω/cm^2 (after BDNF modification), and this directly correlates to an observed decrease in the charge transfer. Charge transfer resistance increases because the bare gold electrode becomes partially passivated and this correspondingly limits the ability of the redox probe to access its surface.

Potentiostatic synthesis of the polymer, PmPD, from the functional monomer solution was then carried out while paying attention to the polymerization parameters such as: applied charge density, and applied potential. Prior to the potentiostatic deposition, the oxidation window of mPD was first determined via CV to obtain the optimum applied potential for polymer synthesis. From the plot in Fig. 3.3a, we observe that the oxidation potential window of mPD lies from 400 mV to 900 mV. Therefore, for potentiostatic deposition, 600mV was adopted as applied potential, though being a

little higher than the $E_{1/2}$ potential (560 mV) of mPD [115]. A similar work on NF-protein imprinted polymers was done using this potential for mPD electrodeposition [15].

For optimization of the thickness of the polymer film, BDNF-MIP and NIP couples were synthesized using charge density of 1 and 2 mC/cm^2 and the rebinding experiments were carried out. The imprinting factor (IF) values calculated by Eq. 2.3 were then compared (Fig. 3.3b). As it can be seen, the polymer film prepared with a charge density of 2 mC/cm^2 had higher IF value which meant it possessed more binding sites within its matrix and could adsorb BDNF more when compared to the film synthesized with a charge density of 1 mC/cm^2. This film had a thickness of 4.7 nm [15] and it was considered as optimum because according to the surface imprinting strategy employed in this work, at this thickness, the polymer film will confine around the protein's median dimension and as such, extraction of the protein from the matrix of the synthesized film to leave a selective molecular cavity can be done effectively.

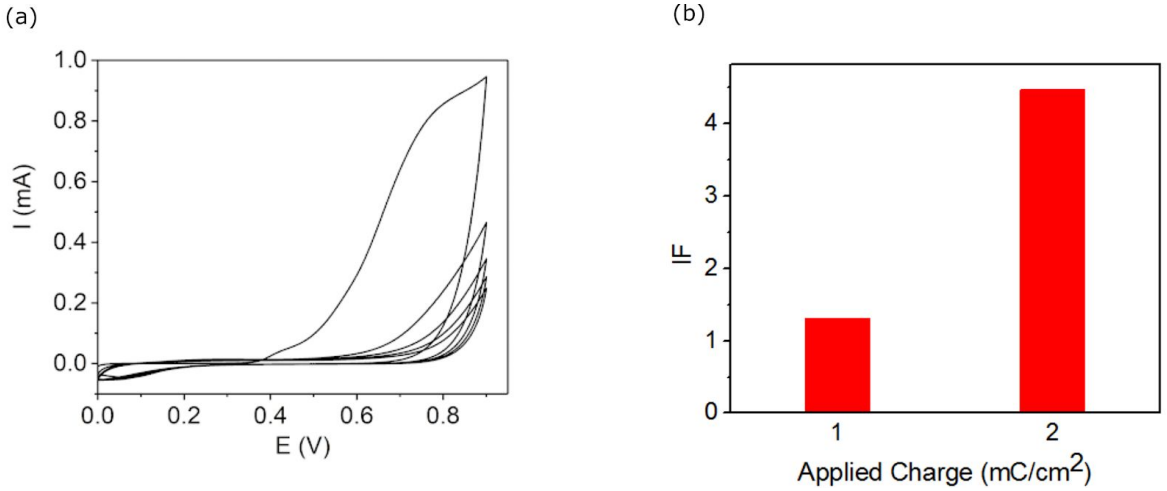

Figure 3.3 (a) Cyclic voltammograms in the range 0-900 mV (gold slide electrode as WE, Ag/AgCl/KCl as RE, and spiral shaped Pt as AE) of 10 mM mPD in PBS. (b) IF values from adsorption curves on BDNF-MIP and-NIP synthesized using charge density of 1 mC/cm^2 and 2 mC/cm^2 on the WE surface of TFE

After polymerization, the entrapped template molecules must be removed from the polymer film and solvent extraction is the common method applied at this stage. This is also referred to as the 'washing out process'. Here, we subject the TFE coated with polymer film firstly to a solvent, which is capable of cleaving the covalent -S-S- bond of the linker DTSSP, and then another solvent, which cleaves the non-covalent hydrogen bonds and ionic bonds existing between carboxyl group of amino acids of the protein and amino group of the polymer matrix and disintegrates the protein from the polymer without degenerating the integrity of the polymer film.

For this aim, we incubated the BDNF-PmPD-modified TFE firstly in a 0.1 M ME solution and then, in a 3 M AA solution and the changes in charge transfer at the electrode/electrolyte interface were electrochemically monitored by CV and EIS. The resulting BDNF-MIP film was further incubated in PBS solution before stabilization by DPV in probe solution.

We assumed that after the template molecules have been removed, the imprinted cavities should be exposed and should permit the diffusion of the ions of the redox probe resulting in an increase of the redox peak current.

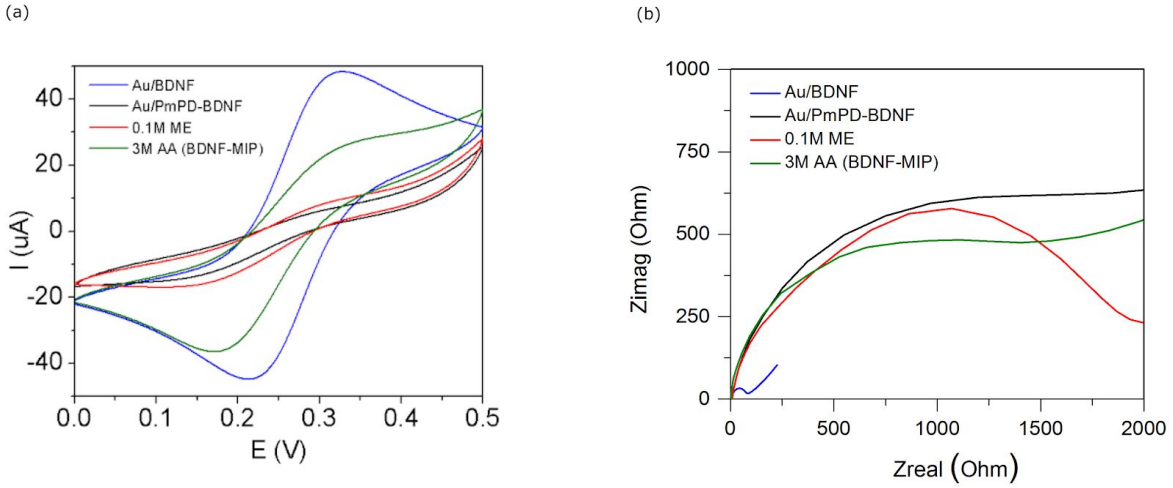

Figure 3.4 (a) CV and (b) EIS measurements showing washing out steps of the synthesized PmPD-BDNF on WE of TFE in 1 M KCl solution containing 4 mM of the redox probe $K_3[Fe(CN)_6]/K_4[Fe(CN)_6]$

In Fig. 3.4a, we observe that the Au electrode modified with BDNF (Au/BDNF) shows a reversible current peak for the redox pair which demonstrates a diffusion-controlled electron transfer reaction. After electropolymerization, we observe the absence of well-defined current peaks on the cyclic voltammogram of Au/PmPD-BDNF modified electrode. This is indicative of a major hindrance to the charge-transfer reaction involving the redox pair resulting from blocking of the surface via the formation of the polymer layer. After using ME as a washing out solvent on the Au/PmPD-BDNF, we also observe that there is no significant change in the current peak comparable to that observed in Au/PmPD-BDNF, indicating that the even though disulphide bonds of the cross linker were cleaved by the action of ME, the protein was still entrapped within the polymer matrix and as a result the presence of surface blocking of the current. Lastly, after AA application, we notice the presence of current transport on the electrode surface. Washing out of the entrapped template molecule from the matrix of PmPD-BDNF leads to the formation of BDNF-MIP. It is pertinent to note that the electronic current observed at the electrode surface after AA action appears lower than that of Au/BDNF, because it undoubtedly informs us that the electrode surface, there

is still presence of the polymer film and also that the polymer surface is not completely blocked, since current can still be observed.

For the EIS spectra, the charge transfer resistance was estimated from the width of the Nyguist plot (Fig. 3.4b). As can be seen, the width of the semicircle increased from 4.176 kΩ/cm^2 (the BDNF-modified Au surface) to 73.656 kΩ/cm^2 (electrodeposited PmPD). We then observe a decrease in the semicircle width to 31.184 kΩ/cm^2 after ME cleavage and lastly 21.108 kΩ/cm^2 after WO with 3M AA. This increase and decrease directly correlates to an observed change in the charge transfer. Charge transfer resistance increases by reason of non-conductive PmPD electrodeposition on the gold surface of WE, and then decreases with the protein cleavage and washing out steps.

3.3 Rebinding study

3.3.1 Electrochemical measurements

BDNF-MIP capability to absorb the target analyte (BDNF) was also studied. We incubated the BDNF-MIP-modified TFE in various concentrations of BDNF solution and monitored the resulting changes in charge transfer by DPV in redox probe solution (Fig. 3.5a). The sensor was first incubated in a blank PBS solution to obtain a reference baseline for the subsequent BDNF concentration measurements. We observe that the current peak reduces with increasing concentration of BDNF, which suggests gradual blocking of the ions from migrating from the solution through the exposed MIP cavities. Fig. 3.5b is the normalized current response (normalized by PBS buffer) which has an inverse relationship with the actual measurement i.e the normalized response increases on increased concentration of BDNF.

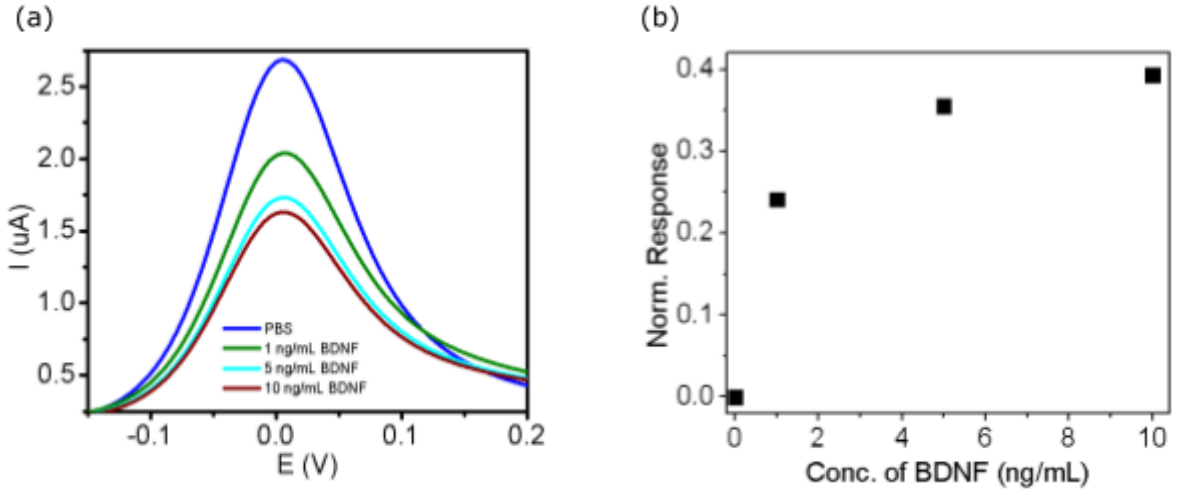

Figure 3.5 (a) DPV current peaks and (b) normalized DPV current peak responses, obtained after incubation of BDNF-MIP sensors in different BDNF concentrations in PBS

3.3.2 Binding isotherms

The values of DPV normalized responses were used to plot the adsorption isotherms for BDNF-MIP and BDNF-NIP towards BDNF (Fig. 3.6). Fitting of these isotherms to Langmuir adsorption model (Eq. 2.2) allowed estimations of the values of saturated response (A_{sat}) for BDNF-MIP and NIP being 0.510 and 0.099, respectively. The imprinting factor (IF) calculated as the ratio between saturated response on BDNF-MIP and -NIP was estimated to be approximately 5.12. This translates to BDNF-MIP having more binding sites with high affinity available in its matrix towards BDNF, its target molecule, and as such is capable of adsorbing BDNF 5.12 times more as compared to the reference, BDNF-NIP.

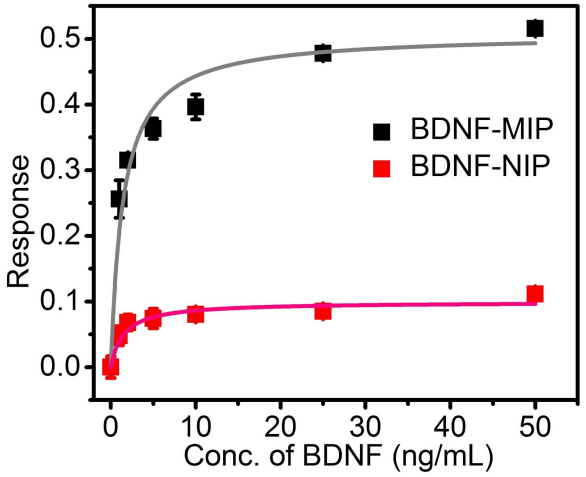

Figure 3.6 BDNF adsorption isotherms on the BDNF-MIP (grey), and BDNF-NIP (red). Saturated response values on BDNF-MIP and BDNF-NIP are 0.510 and 0.099 respectively

3.3.3 Selectivity study

The selectivity of prepared BDNF-MIP was studied by evaluating its capability to bind the target protein and the non-target or interfering proteins such as CDNF, MANF, and CD48 which different in terms of size and isoelectric point (pI) from BDNF. MANF and CDNF, the NF family proteins, were selected because of their always being present in human serum and therefore are capable of interfering with the sensor response just like the target protein (BDNF). CD48 was selected because it has a similar pI value with BDNF and is also present in serum, although both proteins have different molecular weights. The sensor selectivity was first studied in the absence of any background protein. Therefore, for this study, we placed the sensor to interact with both different concentrations BDNF and the non-target proteins in PBS buffer solution. For this purpose, different concentrations of the proteins in the range of 1 – 50 ng/mL were applied. Findings of this study revealed that BDNF-MIP/TFE sensors gave a higher response to BDNF than to the other non-target proteins (Fig. 3.7a). We

observed that with increasing protein concentration, the differences in sensor responses after interaction with BDNF and the non-target proteins also increased. Already at the first concentration (1 ng/mL), BDNF response was approximately five times higher as compared to the other proteins. On the other hand, for BDNF-NIP/TFE sensor, the responses of both BDNF and the non-target proteins remained approximately constant for all proteins at or below the level of BDNF for all tested concentrations with a slight increase observed already at 10 ng/mL concentration (Fig. 3.7b).

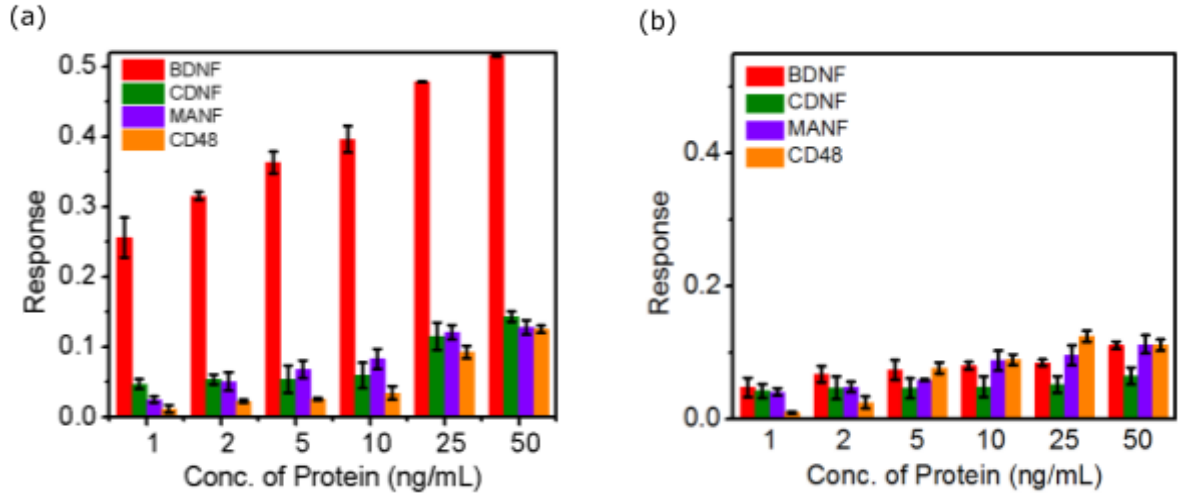

Figure 3.7 The selectivity test of (a) BDNF-MIP and (b) BDNF-NIP towards BDNF, MANF, CDNF and CD48 conducted through incubation in 1 – 50 ng/mL solutions of the various proteins in PBS

Table 3.2 Selectivity factor values of the different proteins used in the selectivity experiment

Protein	A_{sat}		α
	MIP	NIP	
BDNF	0.51	0.10	1.00
CDNF	0.05	0.05	5.12
MANF	0.09	0.10	5.69
CD48	0.02	0.16	39.4

From the selectivity experiments performed on both BDNF-MIP and NIP surfaces, the binding isotherms were plotted and fitted to the Langmuir model (Eq. 2.2). Subsequently, the A_{sat} values obtained on both polymer films for BDNF and the non-target proteins (MANF, CDNF and CD48), were used to calculate their respective imprinting factors ($IF'_{non\text{-}target}$) and selectivity factors (α) (Eq. 2.4). In general, a higher α value means lower selectivity (or lower molecular recognition ability) of the BDNF-MIP film towards the individual particular non-target protein molecule and vice versa. From table 3.2 above, we see that BDNF-MIP exhibits the highest selective recognition towards BDNF as compared to other analytes (α for BDNF=1.00). Although both CDNF and MANF have some close similarities to BDNF (Fig. 1.5), BDNF-MIP

demonstrated about five times (α for CDNF=5.12, MANF=5.69) more preferential recognition towards BDNF than these analogues. Additionally, CD48 with the highest value of α was seen to be the least selectively recognized protein by the BDNF-MIP film.

3.3.4 Determination of limit of detection

Furthermore, to determine the analytical limits for the BDNF-MIP sensor we carried out more rebinding experiments using lower concentration range (0 - 40 pg/ml) of the analyte. However, since the sensor is intended to be used in human serum that consists other interfering analytes, the analyte solutions were prepared in the presence of 0.8 mg/mL HSA concentration being the most abundant protein in human serum.

This concentration of HSA was determined by direct dilution in PBS (approximately 62 times) of normal serum concentration of HSA (35-50 mg/mL) to a concentration where BDNF's effect i.e. its response on the sensor, is apparently measurable in the range of 1 ng/mL and the linear regression plot was obtained (Fig. 3.8). With the BDNF concentration varying from 0 to 40 pg/ml while HSA concentration in solution was kept constant, the sensor produced a quasi-linear response. For the different BDNF concentrations tested within this range, the the coefficient of determination, R-squared, being equal to 0.997 was obtained by the linear regression, and LoD and LoQ values, 5.2 pg/ml and 17.3 pg/ml respectively calculated from the equations below (Eq. 3.2 and 3.3) where SD is the standard deviation.

$$LoD=3\cdot SD/Slope \quad (3.2)$$

$$LoQ=10\cdot SD/Slope \quad (3.3)$$

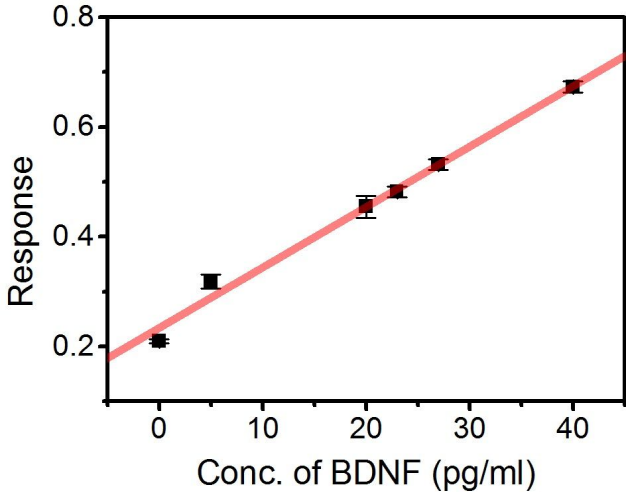

Figure 3.8 The linear regression plot showing BDNF-MIP/TFE sensor responses at different concentrations of BDNF and 0.8 mg/mL HSA in PBS

4. CONCLUSIONS

This thesis supports and provides evidence of the possibility of combining a highly selective and robust BDNF-MIP with a TFE for the electrochemical label-free detection and analysis of BDNF. BDNF, being an important NF protein whose concentration in serum has been directly correlated with the neurological disease state of patients, was selected as target analyte. TFE was selected as a miniaturized, inexpensive electrochemical sensor platform. To prepare a BDNF-MIP on TFE, an electrochemical surface imprinting approach was employed as it created the possibility to develop thin film imprinted polymers with cavities on or close to the surface of the polymer directly on the sensor surface. As a result, these conclusions were drawn from this work:

1. Molecular docking studies supported the selection of meta-phenylenediamine (mPD) as an appropriate functional monomer for the electropolymerization of thin film BDNF-containing polymers.
2. BDNF-MIP electrosynthesis was successfully optimized on the TFE sensor surface. mPD electrochemical polymerization was carried out at potentiostatic mode with a potential of 600 mV(vs Ag/AgCl) and charge density of 2 mC/cm^2, resulting in a homogeneous BDNF-PmPD film on the WE surface of TFE. This was followed by a rigorous 18-hour washing out procedure using mercaptoethanolic and acetic acid solvents to form the BDNF-MIP.
3. Langmuir adsorption model was used to best describe the adsorption of BDNF on BDNF-MIP. The IF value, based on saturated response's ratio, of BDNF on both BDNF-MIP and NIP surfaces was estimated at 5.12 which translates to BDNF-MIP having more binding sites in its matrix than BDNF-NIP and therefore demonstrated a greater adsorption capacity towards BDNF.
4. BDNF-MIP/TFE sensors exhibited significantly higher molecular recognition ability towards BDNF in comparison with other proteins CDNF, MANF and CD48. The sensor's molecular recognition ability, given by the selectivity factor (α), was found to be 5.12, 5.69 and 39.4 times lower for CDNF, MANF and CD48 respectively, than it was for BDNF.
5. BDNF-MIP/TFE sensor showed an outstanding LoD of 5.2 pg/mL for BDNF in the simulated serum solution (PBS containing HSA) and so, these inferences were made;
    - For BDNF ELISA kits, the LoD is approximately 12.2 pg/mL under serum conditions [116]. Therefore, since the LoD of BDNF for this sensor was determined in a simulated serum solution, and was found to be approximately two times lower than that of ELISA, the BDNF-MIP/TFE sensor exhibited impressive analytical performance.

- Furthermore, since serum BDNF concentration in neurologic diseased patients lie approximately within the range 10 times lower than 8 - 40 ng/mL, with our BDNF-MIP/TFE sensor, we will be able to measure serum concentration of BDNF in these disease conditions.

SUMMARY

Neurodegenerative disorders (NDs), which was believed to be associated only with the elderly, is now increasingly becoming prevalent in young people. Brain-derived neurotrophic factor (BDNF), a neurotrophic factor protein whose serum concentration, has a correlation with the neurodegenerative disordered state of an individual was seen to have a significantly lower serum concentration in diseased patients than in normal healthy patients. Hence, there is a need to clinically detect and quantify BDNF concentration in serum in order to help curb the prevalence and early onset of growing neurologic disorders especially in the young people. Currently, ELISA, Liquid Chromatography-Mass Spectrometry among others are methods used for BDNF detection and quantification with outstanding precision. These methods however require quite a lot of strict standard operating procedures, are relatively expensive and in some cases, require specialized operation of their systems which makes them not so feasible for rapid, on-the-spot, analysis. Therefore, sensors modified with synthetic receptors as recognition elements which are cheap, easy to prepare and stable, as compared to the biological receptors can be a prospective alternative analytical tool for BDNF rapid detection.

These synthetic receptors developed by virtue of molecular imprinting technology and known to possess inexpensive fabrication, excellent recognition for the target molecules for which they were made, good stability in both high and low pH and temperature conditions are called Molecularly imprinted polymers (MIPs). MIP films have shown successful application in biosensing, drug delivery, environmental analysis, therapeutic monitoring.

The goal of this thesis work was to prepare a BDNF-MIP film interfaced with a TFE as an inexpensive and miniaturized electrochemical sensor platform and to study the resulting BDNF-MIP/TFE sensor in terms of its sensitivity to and selectivity for BDNF.

Electrochemical surface imprinting approach was adapted for direct synthesis of BDNF-MIP on TFE sensor surface (BDNF-MIP/TFE). Polymer electrosynthesis was done potentiostatically at a potential of 600 mV (vs Ag/AgCl) and charge density of 2 mC/m^2. Afterwards, BDNF was successfully removed from the polymer matrix after washing the polymer in both mercaptoethanolic and acidic solutions for a total of 18 hours. The resulting BDNF-MIP showed quite high adsorption capacity towards BDNF, estimated by the imprinting factor (IF) of 5.12 and it also demonstrated high selectivity for BDNF when compared with other closely related neurotrophic factors and serum protein molecules. Notwithstanding, BDNF-MIP/TFE sensor was also able to detect BDNF in the presence of an interfering protein, HSA, with a LoD value of 5.2

pg/mL (whereas for ELISA kits designed for BDNF, their LoD is approximately 12.2 pg/mL).

To summarize, a BDNF-MIP/TFE sensor capable of selective detection of BDNF protein in artificial serum was successfully fabricated using an electrochemical surface imprinting synthesis strategy. It is of vital importance to note that this possibility to integrate BDNF-MIP with thin film electrode sensors demonstrates great potential for prospective development of novel portable and robust point of care (PoC) devices for analytical sensing and real time diagnosis/prognosis of NDs in patients using their sera.

LIST OF REFERENCES

[1] K. P. Muliyala and M. Varghese, "The complex relationship between depression and dementia," *Ann. Indian Acad. Neurol.*, vol. 13, no. Suppl2, p. S69, 2010.

[2] J. M. Burns, G. Andrews, and M. Szabo, "Depression in young people: what causes it and can we prevent it?," *Med. J. Aust.*, vol. 177, pp. S93–S96, 2002.

[3] G. D. Yancopoulos *et al.*, "Neurotrophic factors, their receptors, and the signal transduction pathways they activate," in *Cold Spring Harbor symposia on quantitative biology*, 1990, vol. 55, pp. 371–379.

[4] O. V. Forlenza *et al.*, "Lower cerebrospinal fluid concentration of brain-derived neurotrophic factor predicts progression from mild cognitive impairment to Alzheimer's disease," *Neuromolecular Med.*, vol. 17, no. 3, pp. 326–332, 2015.

[5] M. Balietti, C. Giuli, and F. Conti, "Peripheral blood brain-derived neurotrophic factor as a biomarker of Alzheimer's disease: are there methodological biases?," *Mol. Neurobiol.*, vol. 55, no. 8, pp. 6661–6672, 2018.

[6] G. Ertürk and B. Mattiasson, "Molecular imprinting techniques used for the preparation of biosensors," *Sensors*, vol. 17, no. 2, p. 288, 2017.

[7] A. Tretjakov, V. Syritski, J. Reut, R. Boroznjak, O. Volobujeva, and A. Öpik, "Surface molecularly imprinted polydopamine films for recognition of immunoglobulin G," *Microchim. Acta*, vol. 180, no. 15–16, pp. 1433–1442, 2013.

[8] M. Kempe and K. Mosbach, "Separation of amino acids, peptides and proteins on molecularly imprinted stationary phases," *J. Chromatogr. A*, vol. 691, no. 1–2, pp. 317–323, 1995.

[9] M. Kempe, M. Glad, and K. Mosbach, "An approach towards surface imprinting using the enzyme ribonuclease A," *J. Mol. Recognit.*, vol. 8, no. 1-2, pp. 35–39, 1995.

[10] K. Sreenivasan, "Synthesis and evaluation of molecularly imprinted polymers for nucleic acid bases using aniline as a monomer," *React. Funct. Polym.*, vol. 67, no. 10, pp. 859–864, Oct. 2007, doi: 10.1016/j.reactfunctpolym.2007.05.017.

[11] M. J. Whitcombe *et al.*, "The rational development of molecularly imprinted polymer-based sensors for protein detection," *Chem. Soc. Rev.*, vol. 40, no. 3, pp. 1547–1571, 2011.

[12] H. Nishino, C.-S. Huang, and K. J. Shea, "Selective protein capture by epitope imprinting," *Angew. Chem. Int. Ed.*, vol. 45, no. 15, pp. 2392–2396, 2006.

[13] H. F. EL-Sharif, H. Aizawa, and S. M. Reddy, "Spectroscopic and quartz crystal microbalance (QCM) characterisation of protein-based MIPs," *Sens. Actuators B Chem.*, vol. 206, pp. 239–245, 2015.

[14] M. Bosserdt *et al.*, "Microelectrospotting as a new method for electrosynthesis of surface-imprinted polymer microarrays for protein recognition," *Biosens. Bioelectron.*, vol. 73, pp. 123–129, 2015.

[15] A. Kidakova, R. Boroznjak, J. Reut, A. Öpik, M. Saarma, and V. Syritski, "Molecularly imprinted polymer-based SAW sensor for label-free detection of cerebral dopamine neurotrophic factor protein," *Sens. Actuators B Chem.*, vol. 308, p. 127708, Apr. 2020, doi: 10.1016/j.snb.2020.127708.

[16] M. Kerschensteiner, C. Stadelmann, G. Dechant, H. Wekerle, and R. Hohlfeld, "Neurotrophic cross-talk between the nervous and immune systems: implications for neurological diseases," *Ann. Neurol. Off. J. Am. Neurol. Assoc. Child Neurol. Soc.*, vol. 53, no. 3, pp. 292–304, 2003.

[17] A. Kidakova, J. Reut, R. Boroznjak, A. Öpik, and V. Syritski, "Advanced sensing materials based on molecularly imprinted polymers towards developing point-of-care diagnostics devices.," *Proc. Est. Acad. Sci.*, vol. 68, no. 2, 2019.

[18] S. Cosnier and M. Holzinger, "Electrosynthesized polymers for biosensing," *Chem. Soc. Rev.*, vol. 40, no. 5, pp. 2146–2156, 2011.

[19] C. Malitesta, E. Mazzotta, R. A. Picca, A. Poma, I. Chianella, and S. A. Piletsky, "MIP sensors–the electrochemical approach," *Anal. Bioanal. Chem.*, vol. 402, no. 5, pp. 1827–1846, 2012.

[20] C. Malitesta, I. Losito, and P. G. Zambonin, "Molecularly imprinted

electrosynthesized polymers: new materials for biomimetic sensors," *Anal. Chem.*, vol. 71, no. 7, pp. 1366–1370, 1999.
[21] A. Tretjakov, V. Syritski, J. Reut, R. Boroznjak, and A. Öpik, "Molecularly imprinted polymer film interfaced with Surface Acoustic Wave technology as a sensing platform for label-free protein detection," *Anal. Chim. Acta*, vol. 902, pp. 182–188, Jan. 2016, doi: 10.1016/j.aca.2015.11.004.
[22] M. V. Polyakov, "Adsorption properties and structure of silica gel," *Zhur Fiz Khim*, vol. 2, pp. 799–805, 1931.
[23] L. Pauling and D. H. Campbell, "The production of antibodies in vitro," *Science*, vol. 95, no. 2469, pp. 440–441, 1942.
[24] A. J. P. Martin, *The development of partition chromatography, Nobel Lecture, December 12, 1952. Nobel lectures, chemistry 1942–1962*. Elsevier, Amsterdam, 1964.
[25] J. L. Morrison, M. Worsley, D. R. Shaw, and G. W. Hodgson, "The nature of the specificity of adsorption of alkyl orange dyes on silica gel," *Can. J. Chem.*, vol. 37, no. 12, pp. 1986–1995, 1959.
[26] G. Wuff and A. Sarhan, "The use of polymers with enzyme-analogous structures for the resolution of racemate," *Angew Chem Int Ed*, vol. 11, pp. 341–345, 1972.
[27] R. Arshady and K. Mosbach, "Synthesis of substrate-selective polymers by host-guest polymerization," *Makromol. Chem.*, vol. 182, no. 2, pp. 687–692, 1981, doi: 10.1002/macp.1981.021820240.
[28] K. Smolinska-Kempisty, A. Guerreiro, F. Canfarotta, C. Cáceres, M. J. Whitcombe, and S. Piletsky, "A comparison of the performance of molecularly imprinted polymer nanoparticles for small molecule targets and antibodies in the ELISA format," *Sci. Rep.*, vol. 6, p. 37638, 2016.
[29] R. Boroznjak, V. Syritski, and A. Öpik, "A Computational Approach for Rational Monomer Selection in Molecularly Imprinted Polymer Synthesis," May 2017, Accessed: May 25, 2020. [Online]. Available: https://digikogu.taltech.ee/et/item/3891f6f8-782b-45aa-ac10-134462ea0943.
[30] P. Zahedi, M. Ziaee, M. Abdouss, A. Farazin, and B. Mizaikoff, "Biomacromolecule template-based molecularly imprinted polymers with an emphasis on their synthesis strategies: a review," *Polym. Adv. Technol.*, vol. 27, no. 9, pp. 1124–1142, 2016.
[31] A. L. Hillberg and M. Tabrizian, "Biomolecule imprinting: Developments in mimicking dynamic natural recognition systems," *Irbm*, vol. 29, no. 2–3, pp. 89–104, 2008.
[32] A. Mujahid, N. Iqbal, and A. Afzal, "Bioimprinting strategies: From soft lithography to biomimetic sensors and beyond," *Biotechnol. Adv.*, vol. 31, no. 8, pp. 1435–1447, 2013.
[33] Y. Ge and A. P. Turner, "Too large to fit? Recent developments in macromolecular imprinting," *Trends Biotechnol.*, vol. 26, no. 4, pp. 218–224, 2008.
[34] Y. Lv, T. Tan, and F. Svec, "Molecular imprinting of proteins in polymers attached to the surface of nanomaterials for selective recognition of biomacromolecules," *Biotechnol. Adv.*, vol. 31, no. 8, pp. 1172–1186, 2013.
[35] P. A. Lieberzeit, S. Gazda-Miarecka, K. Halikias, C. Schirk, J. Kauling, and F. L. Dickert, "Imprinting as a versatile platform for sensitive materials – nanopatterning of the polymer bulk and surfaces," *Sens. Actuators B Chem.*, vol. 111–112, pp. 259–263, Nov. 2005, doi: 10.1016/j.snb.2004.12.064.
[36] A. Rachkov and N. Minoura, "Towards molecularly imprinted polymers selective to peptides and proteins. The epitope approach," *Biochim. Biophys. Acta BBA-Protein Struct. Mol. Enzymol.*, vol. 1544, no. 1–2, pp. 255–266, 2001.
[37] W. Kutner and P. S. Sharma, *Molecularly imprinted polymers for analytical chemistry applications*, vol. 28. Royal Society of Chemistry, 2018.
[38] L. Lvova and D. Kirsanov, "Editorial: Multisensor Systems for Analysis of Liquids and Gases: Trends and Developments," *Front. Chem.*, vol. 6, 2018, doi: 10.3389/fchem.2018.00591.
[39] Y. Ge and A. P. Turner, "Molecularly imprinted sorbent assays: recent developments and applications," *Chem. Eur. J.*, vol. 15, no. 33, pp. 8100–8107,

2009.
[40] A. G. Ayankojo, J. Reut, V. Ciocan, A. Öpik, and V. Syritski, "Molecularly imprinted polymer-based sensor for electrochemical detection of erythromycin," *Talanta*, vol. 209, p. 120502, Mar. 2020, doi: 10.1016/j.talanta.2019.120502.
[41] M. Zayats, A. J. Brenner, and P. C. Searson, "Protein imprinting in polyacrylamide-based gels," *Biomaterials*, vol. 35, no. 30, pp. 8659–8668, Oct. 2014, doi: 10.1016/j.biomaterials.2014.05.079.
[42] R. Boroznjak, J. Reut, A. Tretjakov, A. Lomaka, A. Öpik, and V. Syritski, "A computational approach to study functional monomer-protein molecular interactions to optimize protein molecular imprinting," *J. Mol. Recognit.*, vol. 30, no. 10, p. e2635, 2017, doi: 10.1002/jmr.2635.
[43] V. Pichon and F. Chapuis-Hugon, "Role of molecularly imprinted polymers for selective determination of environmental pollutants—A review," *Anal. Chim. Acta*, vol. 622, no. 1, pp. 48–61, Aug. 2008, doi: 10.1016/j.aca.2008.05.057.
[44] N. Pérez-Moral and A. G. Mayes, "Comparative study of imprinted polymer particles prepared by different polymerisation methods," *Anal. Chim. Acta*, vol. 504, no. 1, pp. 15–21, 2004.
[45] O. Brüggemann, K. Haupt, L. Ye, E. Yilmaz, and K. Mosbach, "New configurations and applications of molecularly imprinted polymers," *J. Chromatogr. A*, vol. 889, no. 1–2, pp. 15–24, 2000.
[46] V. Pichon and F. Chapuis-Hugon, "Role of molecularly imprinted polymers for selective determination of environmental pollutants—a review," *Anal. Chim. Acta*, vol. 622, no. 1–2, pp. 48–61, 2008.
[47] S. Tokonami, H. Shiigi, and T. Nagaoka, "Review: Micro- and nanosized molecularly imprinted polymers for high-throughput analytical applications," *Anal. Chim. Acta*, vol. 641, no. 1, pp. 7–13, May 2009, doi: 10.1016/j.aca.2009.03.035.
[48] N. Pérez-Moral and A. G. Mayes, "MIP formats for analytical applications," *Mol. Imprinting Polym.*, pp. 1–11, 2006.
[49] P.-C. Chou, J. Rick, and T.-C. Chou, "C-reactive protein thin-film molecularly imprinted polymers formed using a micro-contact approach," *Anal. Chim. Acta*, vol. 542, no. 1, pp. 20–25, 2005.
[50] P. S. Sharma, A. Pietrzyk-Le, F. D'souza, and W. Kutner, "Electrochemically synthesized polymers in molecular imprinting for chemical sensing," *Anal. Bioanal. Chem.*, vol. 402, no. 10, pp. 3177–3204, 2012.
[51] A. Thiha and F. Ibrahim, "A Colorimetric Enzyme-Linked Immunosorbent Assay (ELISA) Detection Platform for a Point-of-Care Dengue Detection System on a Lab-on-Compact-Disc," *Sensors*, vol. 15, no. 5, pp. 11431–11441, May 2015, doi: 10.3390/s150511431.
[52] A. Syahir, K. Usui, K. Tomizaki, K. Kajikawa, and H. Mihara, "Label and Label-Free Detection Techniques for Protein Microarrays," *Microarrays*, vol. 4, no. 2, pp. 228–244, Apr. 2015, doi: 10.3390/microarrays4020228.
[53] Q. Q. Wei and T. X. Wei, "A novel method to prepare SPR sensor chips based on photografting molecularly imprinted polymer," *Chin. Chem. Lett.*, vol. 22, no. 6, pp. 721–724, Jun. 2011, doi: 10.1016/j.cclet.2010.11.024.
[54] R. Pernites, R. Ponnapati, M. J. Felipe, and R. Advincula, "Electropolymerization molecularly imprinted polymer (E-MIP) SPR sensing of drug molecules: Pre-polymerization complexed terthiophene and carbazole electroactive monomers," *Biosens. Bioelectron.*, vol. 26, no. 5, pp. 2766–2771, Jan. 2011, doi: 10.1016/j.bios.2010.10.027.
[55] G. Ertürk, H. Özen, M. A. Tümer, B. Mattiasson, and A. Denizli, "Microcontact imprinting based surface plasmon resonance (SPR) biosensor for real-time and ultrasensitive detection of prostate specific antigen (PSA) from clinical samples," *Sens. Actuators B Chem.*, vol. 224, pp. 823–832, Mar. 2016, doi: 10.1016/j.snb.2015.10.093.
[56] A. Kidakova, J. Reut, J. Rappich, A. Öpik, and V. Syritski, "Preparation of a surface-grafted protein-selective polymer film by combined use of controlled/living radical photopolymerization and microcontact imprinting," *React.*

Funct. Polym., vol. 125, pp. 47–56, 2018.
[57] A. Gültekin, G. Karanfil, M. Kuş, S. Sönmezoğlu, and R. Say, "Preparation of MIP-based QCM nanosensor for detection of caffeic acid," *Talanta*, vol. 119, pp. 533–537, Feb. 2014, doi: 10.1016/j.talanta.2013.11.053.
[58] A. G. Ayankojo, J. Reut, A. Öpik, A. Tretjakov, and V. Syritski, "Enhancing binding properties of imprinted polymers for the detection of small molecules.," *Proc. Est. Acad. Sci.*, vol. 67, no. 2, 2018.
[59] T.-Y. Lin, C.-H. Hu, and T.-C. Chou, "Determination of albumin concentration by MIP-QCM sensor," *Biosens. Bioelectron.*, vol. 20, no. 1, pp. 75–81, Jul. 2004, doi: 10.1016/j.bios.2004.01.028.
[60] Z. Mazouz *et al.*, "Highly Selective Polypyrrole MIP-Based Gravimetric and Electrochemical Sensors for Picomolar Detection of Glyphosate," *Sensors*, vol. 17, no. 11, p. 2586, Nov. 2017, doi: 10.3390/s17112586.
[61] A. G. Ayankojo *et al.*, "Molecularly imprinted polymer integrated with a surface acoustic wave technique for detection of sulfamethizole," *Anal. Chem.*, vol. 88, no. 2, pp. 1476–1484, 2016.
[62] M. Vestergaard, K. Kerman, and E. Tamiya, "An overview of label-free electrochemical protein sensors," *Sensors*, vol. 7, no. 12, pp. 3442–3458, 2007.
[63] T. P. Nguy, T. Van Phi, D. T. N. Tram, K. Eersels, P. Wagner, and T. T. N. Lien, "Development of an impedimetric sensor for the label-free detection of the amino acid sarcosine with molecularly imprinted polymer receptors," *Sens. Actuators B Chem.*, vol. 246, pp. 461–470, Jul. 2017, doi: 10.1016/j.snb.2017.02.101.
[64] J. Krejci, J. Maly, and R. Stejskalova, *Nanostructured working electrode of an electrochemical sensor, method of manufacturing thereof and sensor containing this working electrode*. Google Patents, 2010.
[65] Z. Taleat, A. Khoshroo, and M. Mazloum-Ardakani, "Screen-printed electrodes for biosensing: a review (2008–2013)," *Microchim. Acta*, vol. 181, no. 9, pp. 865–891, Jul. 2014, doi: 10.1007/s00604-014-1181-1.
[66] "EmStat3 Blue," *PalmSens*. https://www.palmsens.com/product/emstat-blue/ (accessed May 25, 2020).
[67] A. Fernández-la-Villa, D. F. Pozo-Ayuso, and M. Castaño-Álvarez, "Microfluidics and electrochemistry: an emerging tandem for next-generation analytical microsystems," *Curr. Opin. Electrochem.*, vol. 15, pp. 175–185, Jun. 2019, doi: 10.1016/j.coelec.2019.05.014.
[68] G.-P. Nikoleli, C. G. Siontorou, D. P. Nikolelis, S. Bratakou, S. Karapetis, and N. Tzamtzis, "Chapter 13 - Biosensors Based on Microfluidic Devices Lab-on-a-Chip and Microfluidic Technology," in *Nanotechnology and Biosensors*, D. P. Nikolelis and G.-P. Nikoleli, Eds. Elsevier, 2018, pp. 375–394.
[69] A. Fernández-la-Villa, D. F. Pozo-Ayuso, and M. Castaño-Álvarez, "Microfluidics and electrochemistry: an emerging tandem for next-generation analytical microsystems," *Curr. Opin. Electrochem.*, vol. 15, pp. 175–185, Jun. 2019, doi: 10.1016/j.coelec.2019.05.014.
[70] "MicruX Technologies | Electrochemistry & Microfluidics." https://www.micruxfluidic.com/en/ (accessed May 25, 2020).
[71] M. W. Gonzalez and M. G. Kann, "Chapter 4: Protein Interactions and Disease," *PLOS Comput. Biol.*, vol. 8, no. 12, p. e1002819, Dec. 2012, doi: 10.1371/journal.pcbi.1002819.
[72] J. T. Busher, "Serum albumin and globulin," *Clin. Methods Hist. Phys. Lab. Exam.*, vol. 3, pp. 497–9, 1990.
[73] R. C. Malenka, E. J. Nestler, and S. E. Hyman, "Atypical neurotransmitters," *Mol. Neuropharmacol. Found. Clin. Neurosci.*, pp. 199–215, 2009.
[74] D. K. Binder and H. E. Scharfman, "Brain-derived neurotrophic factor," *Growth Factors Chur Switz.*, vol. 22, no. 3, p. 123, 2004.
[75] E. M. JOHNSON JR and M. H. TUSZYNSKI, "Neurotrophic factors," in *CNS Regeneration*, Elsevier, 2008, pp. 95–144.
[76] F. Karege, G. Perret, G. Bondolfi, M. Schwald, G. Bertschy, and J.-M. Aubry, "Decreased serum brain-derived neurotrophic factor levels in major depressed patients," *Psychiatry Res.*, vol. 109, no. 2, pp. 143–148, 2002.

[77] B. Lima Giacobbo, J. Doorduin, H. C. Klein, R. A. J. O. Dierckx, E. Bromberg, and E. F. J. de Vries, "Brain-Derived Neurotrophic Factor in Brain Disorders: Focus on Neuroinflammation," *Mol. Neurobiol.*, vol. 56, no. 5, pp. 3295–3312, May 2019, doi: 10.1007/s12035-018-1283-6.
[78] Y.-A. Barde, D. Edgar, and H. Thoenen, "Purification of a new neurotrophic factor from mammalian brain.," *EMBO J.*, vol. 1, no. 5, pp. 549–553, 1982.
[79] C. Hölscher, "Growth Factors: Neuronal Atrophy," 2017.
[80] R. Yoshimura, H. Hori, A. Sugita-Ikenouchi, W. Umene-Nakano, A. Katsuki, and J. Nakamura, "Serum Brain–Derived Neurotrophic Factor Levels at 6 Months After Remission Are Not Associated With Subsequent Depressive Episodes," *J. Clin. Psychopharmacol.*, vol. 33, no. 1, pp. 142–143, 2013.
[81] M. Miranda, J. F. Morici, M. B. Zanoni, and P. Bekinschtein, "Brain-derived neurotrophic factor: a key molecule for memory in the healthy and the pathological brain," *Front. Cell. Neurosci.*, vol. 13, p. 363, 2019.
[82] K. Toyooka *et al.*, "Decreased levels of brain-derived neurotrophic factor in serum of chronic schizophrenic patients," *Psychiatry Res.*, vol. 110, no. 3, pp. 249–257, 2002.
[83] U. E. Lang, R. Hellweg, and J. Gallinat, "BDNF Serum Concentrations in Healthy Volunteers are Associated with Depression-Related Personality Traits," *Neuropsychopharmacology*, vol. 29, no. 4, pp. 795–798, Apr. 2004, doi: 10.1038/sj.npp.1300382.
[84] V. Shridhar *et al.*, "A gene from human chromosomal band 3p21. 1 encodes a highly conserved arginine-rich protein and is mutated in renal cell carcinomas.," *Oncogene*, vol. 12, no. 9, pp. 1931–1939, 1996.
[85] P. S. Petrova *et al.*, "MANF," *J. Mol. Neurosci.*, vol. 20, no. 2, pp. 173–187, 2003.
[86] M. Airavaara *et al.*, "Mesencephalic astrocyte-derived neurotrophic factor reduces ischemic brain injury and promotes behavioral recovery in rats," *J. Comp. Neurol.*, vol. 515, no. 1, pp. 116–124, 2009.
[87] H. J. Huttunen and M. Saarma, "CDNF protein therapy in parkinson's disease," *Cell Transplant.*, vol. 28, no. 4, pp. 349–366, 2019.
[88] P. Lindholm *et al.*, "MANF is widely expressed in mammalian tissues and differently regulated after ischemic and epileptic insults in rodent brain," *Mol. Cell. Neurosci.*, vol. 39, no. 3, pp. 356–371, 2008.
[89] P. Lindholm *et al.*, "Novel neurotrophic factor CDNF protects and rescues midbrain dopamine neurons in vivo," *Nature*, vol. 448, no. 7149, pp. 73–77, 2007.
[90] P. Lindholm and M. Saarma, "Novel CDNF/MANF family of neurotrophic factors," *Dev. Neurobiol.*, vol. 70, no. 5, pp. 360–371, 2010.
[91] R. Lindström *et al.*, "Characterization of the Structural and Functional Determinants of MANF/CDNF in Drosophila In Vivo Model," *PLoS ONE*, vol. 8, no. 9, Sep. 2013, doi: 10.1371/journal.pone.0073928.
[92] T. Tang, Y. Li, Q. Jiao, X. Du, and H. Jiang, "Cerebral dopamine neurotrophic factor: a potential therapeutic agent for Parkinson's disease," *Neurosci. Bull.*, vol. 33, no. 5, pp. 568–575, 2017.
[93] "Serum Protein Components." https://rockland-inc.com/Serum-Protein-Components.aspx (accessed Mar. 20, 2020).
[94] J. R. Marrack and H. Hoch, "Serum proteins: A review," *J. Clin. Pathol.*, vol. 2, no. 3, p. 161, 1949.
[95] G. Weaving, G. F. Batstone, and R. G. Jones, "Age and sex variation in serum albumin concentration: an observational study," *Ann. Clin. Biochem.*, vol. 53, no. 1, pp. 106–111, 2016.
[96] R. Peralta, *Hypoalbuminemia. Medscape Updated Clinical Reference. 2010*. 2011.
[97] D. E. Staunton and D. A. Thorley-Lawson, "Molecular cloning of the lymphocyte activation marker Blast-1.," *EMBO J.*, vol. 6, no. 12, pp. 3695–3701, 1987.
[98] F. Cunningham *et al.*, "Ensembl 2019," *Nucleic Acids Res.*, vol. 47, no. D1, pp. D745–D751, 2019.
[99] A. Adumitrăchioaie, M. Tertiş, A. Cernat, R. Săndulescu, and C. Cristea,

"Electrochemical methods based on molecularly imprinted polymers for drug detection. A review," *Int J Electrochem Sci*, vol. 13, pp. 2556–2576, 2018.
[100] P. T. Kissinger and W. R. Heineman, "Cyclic voltammetry," *J. Chem. Educ.*, vol. 60, no. 9, p. 702, 1983.
[101] G. A. Mabbott, "An introduction to cyclic voltammetry," *J. Chem. Educ.*, vol. 60, no. 9, p. 697, 1983.
[102] J. R. Macdonald, "Impedance spectroscopy," *Ann. Biomed. Eng.*, vol. 20, no. 3, pp. 289–305, 1992.
[103] N. Elgrishi, K. J. Rountree, B. D. McCarthy, E. S. Rountree, T. T. Eisenhart, and J. L. Dempsey, "A practical beginner's guide to cyclic voltammetry," *J. Chem. Educ.*, vol. 95, no. 2, pp. 197–206, 2018.
[104] A. J. Bard and L. R. Faulkner, "Fundamentals and applications," *Electrochem. Methods*, vol. 2, no. 482, pp. 580–632, 2001.
[105] F. Scholz, *Electroanalytical methods*, vol. 1. Springer, 2010.
[106] E. Laborda, J. González, and Á. Molina, "Recent advances on the theory of pulse techniques: A mini review," *Electrochem. Commun.*, vol. 43, pp. 25–30, Jun. 2014, doi: 10.1016/j.elecom.2014.03.004.
[107] S. Kröger, A. P. F. Turner, K. Mosbach, and K. Haupt, "Imprinted Polymer-Based Sensor System for Herbicides Using Differential-Pulse Voltammetry on Screen-Printed Electrodes," *Anal. Chem.*, vol. 71, no. 17, pp. 3698–3702, Sep. 1999, doi: 10.1021/ac9811827.
[108] B.-Y. Chang and S.-M. Park, "Electrochemical Impedance Spectroscopy," *Annu. Rev. Anal. Chem.*, vol. 3, no. 1, pp. 207–229, Jun. 2010, doi: 10.1146/annurev.anchem.012809.102211.
[109] R. Schweiss, C. Werner, and W. Knoll, "Impedance spectroscopy studies of interfacial acid–base reactions of self-assembled monolayers," *J. Electroanal. Chem.*, vol. 540, pp. 145–151, Jan. 2003, doi: 10.1016/S0022-0728(02)01303-7.
[110] "Electrochemical Impedance Analysis of Lithium Cobalt Oxide Batteries." https://ufdc.ufl.edu/UFE0043492/00001 (accessed May 26, 2020).
[111] H. Liu *et al.*, "Microporous layer degradation in polymer electrolyte membrane fuel cells," *J. Electrochem. Soc.*, vol. 165, no. 6, pp. F3271–F3280, 2018.
[112] G. Weng, E. Wang, F. Chen, H. Sun, Z. Wang, and T. Hou, "Assessing the performance of MM/PBSA and MM/GBSA methods. 9. Prediction reliability of binding affinities and binding poses for protein–peptide complexes," *Phys. Chem. Chem. Phys.*, vol. 21, no. 19, pp. 10135–10145, May 2019, doi: 10.1039/C9CP01674K.
[113] G. M. Morris and M. Lim-Wilby, "Molecular docking," *Methods Mol. Biol. Clifton NJ*, vol. 443, pp. 365–382, 2008, doi: 10.1007/978-1-59745-177-2_19.
[114] D. R. Kryscio, Y. Shi, P. Ren, and N. A. Peppas, "Molecular Docking Simulations for Macromolecularly Imprinted Polymers," *Ind. Eng. Chem. Res.*, vol. 50, no. 24, pp. 13877–13884, Dec. 2011, doi: 10.1021/ie201858n.
[115] J. A. McCleverty and T. J. Meyer, *Comprehensive coordination chemistry II: from biology to nanotechnology*. Elsevier Pergamon, 2004.
[116] "ELISA-Kit-for-Brain-Derived-Neurotrophic-Factor-(BDNF)-SEA011Mi.pdf." Accessed: May 26, 2020. [Online]. Available: http://www.cloud-clone.com/manual/ELISA-Kit-for-Brain-Derived-Neurotrophic-Factor-(BDNF)-SEA011Mi.pdf.